STRUCTURAL BIOLOGY

Molecular mechanisms of metabotropic $GABA_B$ receptor function

Hamidreza Shaye[1,2], Benjamin Stauch[1,2], Cornelius Gati[2,3,4], Vadim Cherezov[1,2,4]*

Metabotropic γ-aminobutyric acid G protein–coupled receptors ($GABA_B$) represent one of the two main types of inhibitory neurotransmitter receptors in the brain. These receptors act both pre- and postsynaptically by modulating the transmission of neuronal signals and are involved in a range of neurological diseases, from alcohol addiction to epilepsy. A series of recent cryo-EM studies revealed critical details of the activation mechanism of $GABA_B$. Structures are now available for the receptor bound to ligands with different modes of action, including antagonists, agonists, and positive allosteric modulators, and captured in different conformational states from the inactive *apo* to the fully active state bound to a G protein. These discoveries provide comprehensive insights into the activation of the $GABA_B$ receptor, which not only broaden our understanding of its structure, pharmacology, and physiological effects but also will ultimately facilitate the discovery of new therapeutic drugs and neuromodulators.

INTRODUCTION

γ-Aminobutyric acid (GABA) is a key neurotransmitter in the central nervous system (CNS) and is responsible for the inhibition of neurons (*1*). In the synaptic cleft, GABA is sensed by two types of receptors, $GABA_A$ and $GABA_B$. Ionotropic $GABA_A$ receptors are pentameric ligand-gated ion channels that mediate fast responses (milliseconds) by counteracting potentials through increasing the Cl^- permeability of the neuronal membrane (*2*, *3*). Metabotropic $GABA_B$ receptors are G protein–coupled receptors (GPCRs), which, on the other hand, elicit slow (hundreds of milliseconds) and sustained activity (*4*) by triggering signal transduction pathways with downstream effectors such as ion channels and adenylyl cyclases, mainly via $G_{i/o}$ proteins (Fig. 1). $GABA_B$ receptors act both pre- and postsynaptically, where they either block neurotransmitter release through the inhibition of voltage-gated Ca^{2+} channels or induce hyperpolarization of the neuron by opening G protein–gated inwardly rectifying K^+ (GIRK) channels (*5*). Given the central role of $GABA_B$ in neurobiology, it is implicated in a broad spectrum of neurological and psychiatric disorders, such as epilepsy (*6*), spasticity (*7*), stress (*8*), sleep disorders (*9*), neuropathic pain (*10*), and depression and anxiety (*11*). $GABA_B$ has also been strongly linked to drug addiction, where the systemic administration of the selective $GABA_B$ agonist baclofen inhibits alcohol, cocaine, morphine, and heroin self-administration in rats (*12*) and is under investigation as a treatment of alcohol addiction in human patients (https://clinicaltrials.gov/ct2/show/NCT02596763).

$GABA_B$, together with metabotropic glutamate (mGlu), calcium sensing (CaS), and taste (TAS) receptors, forms class C of GPCRs (*13*). $GABA_B$ receptor was the first GPCR for which the functional entity was demonstrated to be an obligate heterodimer, consisting of two subunits GB1 and GB2, and each subunit individually is thought to be not capable of signaling (*14*–*16*). Each receptor subunit comprises an extracellular Venus flytrap (VFT) domain, connected by a short linker to the canonical seven-transmembrane domain (TMD). There are two major identified isoforms of GB1: GB1a [961 amino acids, UniProt (*17*) ID Q9UBS5] and GB1b (844 amino acids, UniProt ID O75899), which differ in either the presence (GB1a) or absence (GB1b) of two "sushi" domains (SD1 and SD2) at the N terminus. The main role of the sushi domains is trafficking and cell surface stabilization; heterodimers containing GB1a interact with amyloid precursor protein (APP) directing them into axons of glutamatergic neurons, while both isoforms traffic into dendrites (*18*, *19*). The C termini of both subunits contain a coiled-coil (CC) motif, which has two known functions: The formation of the CC has a positive effect on the heterodimerization of $GABA_B$, while this interaction also masks an endoplasmic reticulum (ER) retention signal on GB1, ensuring that, predominantly, heterodimers are trafficked toward the plasma membrane (*20*). Receptor activation has been proposed to consist of a unique allosteric mechanism, where binding of an agonist in the VFT of GB1 results in a series of conformational rearrangements, which are translated into the TMD of GB2 to trigger G protein signaling (*21*).

Five recent studies have described high-resolution reconstructions of the near full-length $GABA_B$ heterodimer by single-particle cryo–electron microscopy (cryo-EM) (*22*–*26*). In particular, it was possible to map the activation pathway by capturing several discrete conformational states: inactive (*apo* and antagonist bound), two intermediates (agonist bound), active [agonist and positive allosteric modulator (PAM) bound], and active in complex with G protein (agonist, PAM, and G protein bound). These structures provide detailed insights into the unique activation mechanism of $GABA_B$, where upon agonist binding, large conformational rearrangements of the VFTs are translated to the TMDs, ultimately leading to signaling via G proteins.

Despite tremendous efforts to develop novel drugs, only few targeting $GABA_B$ are Food and Drug Administration–approved, one of which is the muscle relaxant baclofen (*27*). Several drug candidates showed promising initial results but were ultimately abandoned due to severe side effects (i.e., seizures, sedation, and respiratory depression) as well as the development of tolerance and dependence. We believe that structural insights in the intricate activation mechanism of $GABA_B$ receptors offer opportunities for pharmaceutical

[1]Department of Chemistry, University of Southern California, Los Angeles, CA, USA. [2]Bridge Institute, Michelson Center for Convergent Biosciences, University of Southern California, Los Angeles, CA, USA. [3]Biosciences Division, SLAC National Accelerator Laboratory, Menlo Park, CA, USA. [4]Department of Biological Sciences, University of Southern California, Los Angeles, CA, USA.
*Corresponding author. Email: cherezov@usc.edu

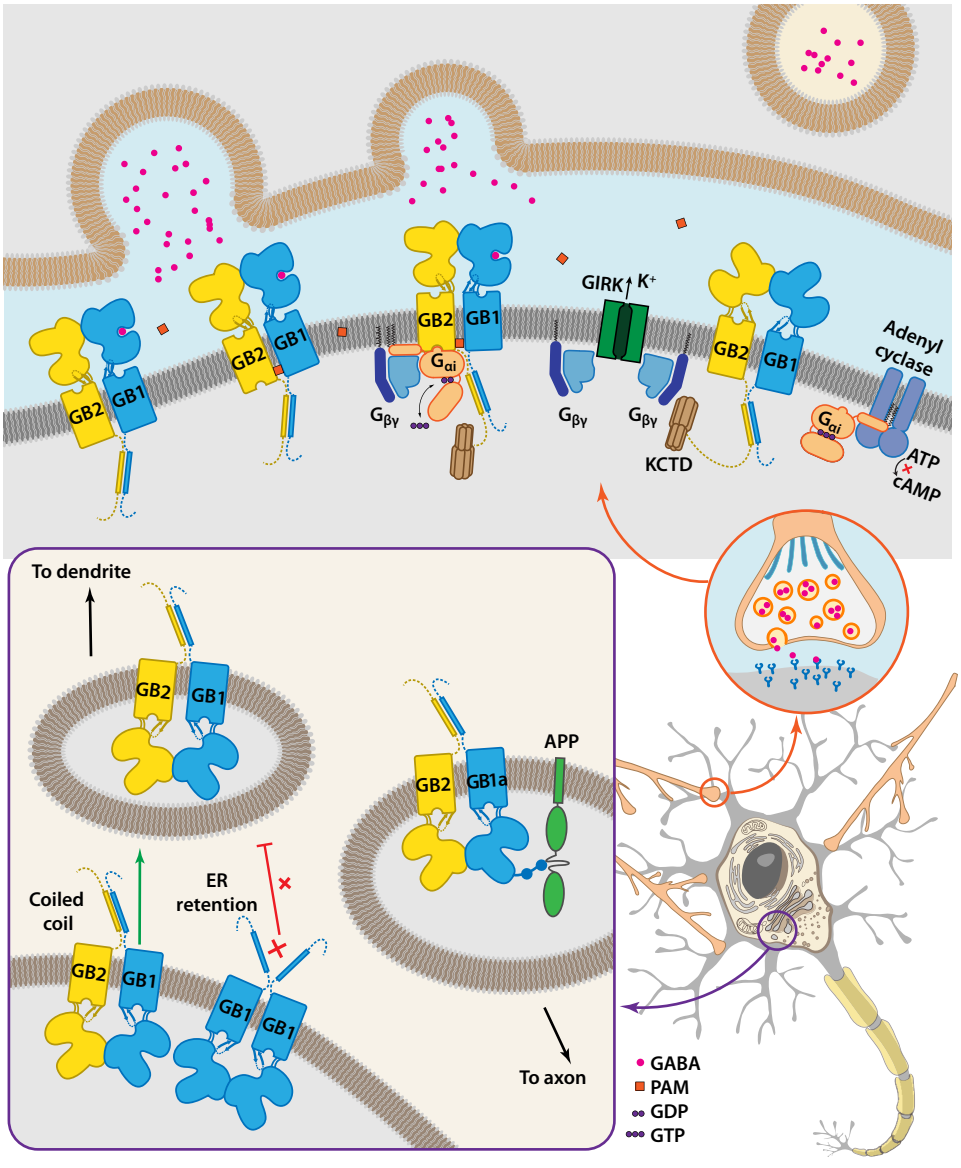

Fig. 1. $GABA_B$ trafficking, downstream effectors, and their physiological function. GB1-GB2 heterodimer assembles in the endoplasmic reticulum (ER) of neurons, facilitated by the formation of C-terminal coiled-coil that masks the GB1 ER retention motif (bottom left). $GABA_B$ heterodimers containing the GB1a isoform with two N-terminal sushi domains interact with amyloid precursor proteins (APPs), which help trafficking them to presynaptic membranes of axons, while both receptors containing GB1a or GB1b populate postsynaptic membranes of dendrites. GABA released in the synaptic cleft binds to GB1 VFT activating the receptor, while binding of PAM at the heterodimeric interface further stabilizes the active state. Heterotrimeric guanosine diphosphate (GDP)–bound G_i protein binds to the intercellular side of GB2 TMD of the activated receptor, leading to GDP to guanosine 5′-triphosphate (GTP) exchange and disassociation of the G_i protein into $G_{\alpha i}$ and $G_{\beta\gamma}$ subunits. $G_{\alpha i}$ inhibits adenylyl cyclase reducing the level of cyclic adenosine 3′,5′-monophosphate (cAMP) in the cell, while $G_{\beta\gamma}$ activates G protein–gated inwardly rectifying K^+ (GIRK) channel, inducing outflow of K^+ ions. Potassium channel tetramerization domain (KCTD) proteins assemble on the C terminus of GB2 and modulate the kinetics of $GABA_B$ signaling by sequestering $G_{\beta\gamma}$ subunits from GIRKs.

intervention by compounds with functional properties distinct from classical agonists, particularly by allosteric modulators.

In this review, we will describe our current understanding of the unique activation mechanism of $GABA_B$ on a molecular level, which provides fundamental insights into the biology of this important neurotransmitter receptor. We will emphasize the structural aspects of receptor activation while also placing these novel findings in the context of physiology, pathology, and drug development.

HISTORICAL PERSPECTIVE AND MAJOR MILESTONES OF $GABA_B$ RESEARCH

While known as a metabolite in plants and bacteria since the beginning of the 20th century, GABA was not actively studied until its discovery as the major amine present in the brain in 1950 (*28*, *29*). The inhibitory function of GABA was first proposed in the late 1950s (*30*); however, its role remained controversial for another decade. Since the late 1960s and the 1970s, research had accelerated,

firmly establishing GABA as an inhibitory neurotransmitter acting through a receptor (*31*). Eventually, Bowery and colleagues (*32*, *33*) found distinct GABA binding sites in 1980, coining the term $GABA_B$ receptor to distinguish it from the previously known $GABA_A$ receptor. The physiological roles of $GABA_B$ were uncovered in a series of studies in the late 1980s (*34*); however, it has taken another decade to clone the two subunits and establish the heterodimeric nature of the receptor, as reported in three seminal back-to-back publications in 1998 (*14*–*16*). Cloning $GABA_B$ opened up a venue for studying molecular mechanisms of its function, where a high-resolution receptor structure would have been critical but remained elusive, resulting in a divide-and-conquer approach for structure determination. During the past several years, crystallography and nuclear magnetic resonance (NMR) revealed the structure of the VFTs and the details of its orthosteric ligand-binding site (*35*, *36*), the structure of the CC domain that regulates receptor trafficking (*20*), that of the GB2 C-terminal peptide in complex with an auxiliary protein potassium channel tetramerization domain (KCTD) regulating $GABA_B$ signaling (*37*, *38*), and the structure of the sushi domains SD2 (*39*) and SD1 in complex with a peptide derived from soluble amyloid-precursor protein (*40*). Last, 70 years after the discovery of GABA in the brain, five research groups (*22*–*26*) independently determined 12 cryo-EM structures of nearly full-length $GABA_B$ heterodimer in complex with different ligands and in different conformational states (Table 1), shedding light on its molecular mechanisms of signal transduction across the membrane.

STRUCTURE DETERMINATION OF THE FULL-LENGTH $GABA_B$ HETERODIMER

The breakthrough in $GABA_B$ structure determination was enabled by technological advancements in cryo-EM, as well as receptor expression and purification. Most important recent improvements include optimized protocols for cryo-EM sample preparation, particularly using accumulated knowledge of suitable detergents for membrane protein structure determination (*41*), substantially faster data collection strategies by exploiting beam shift (*42*), better access to high-end instrumentation, and markedly improved data processing pipelines (*43*–*45*). Near full-length constructs of GB1 and GB2, lacking the N-terminal sushi domains and flexible C-terminal tails, were transiently coexpressed in insect (Sf9) (*22*, *24*) or mammalian (HEK293GnTI$^-$ or HEK293F) (*23*, *25*, *26*) suspension cells using baculovirus- or polyethylenimine-mediated transfection. Sodium butyrate was added 10 to 18 hours after transfection to increase protein expression in mammalian cells (*23*, *25*, *26*). Cells were harvested 48 hour (Sf9) or 48 to 90 hours [HEK293 (human embryonic kidney 293)] after transfection, and receptors were extracted from isolated membranes using either *n*-dodecyl-β-D-maltopyranoside/cholesteryl hemisuccinate (CHS) (*22*, *24*) or lauryl maltose neopentyl glycol/CHS (*23*, *25*, *26*). The detergents used for extraction were replaced by digitonin (*22*) or glyco-diosgenin/CHS (*24*, *26*) during receptor purification. Solubilized receptors were purified in the presence or absence of the corresponding ligands using dual-affinity chromatography with two different affinity tags (Flag, His, or enhanced green fluorescent protein) situated on GB1 and GB2 subunits, respectively. Park *et al.* (*23*) used ion-exchange chromatography instead of the second affinity purification step. Mao *et al.* (*25*) further assembled and captured $GABA_B$ in complex with a heterotrimeric G_i protein and a stabilizing antibody scFv16. In all cases, purified and concentrated receptors were run through a size exclusion column packed with Superose 6 (or Superose 6 Increase) resin before applying them to EM grids, blotting, and plunge-freezing in liquid ethane (*22*, *24*–*26*) or propane/ethane (*23*). Kim *et al.* (*26*) added 0.1% octyl-β-D-glucoside (OG) to the sample before transferring it to the grids to alleviate the problem of preferred receptor orientation, which often occurs in case of elongated molecules, such as $GABA_B$, trapped in thin ice. Addition of OG results in lowering the surface tension and can lead to increased ice thickness, allowing to capture a broader range of receptor orientations, however, in expense of a higher noise limiting the overall resolution. Despite the variations in the sample preparation protocols and potential limitations due to the use of detergent rather than membrane environment, the $GABA_B$ structures obtained by different groups show remarkable consistency, highlighting the robustness of the applied approaches.

STRUCTURE OF THE $GABA_B$ HETERODIMER

The overall assembly of the $GABA_B$ heterodimer follows the class C GPCR topology of a dimeric receptor with a large extracellular ligand-binding domain (Fig. 2). The N-terminal extracellular domains, each consisting of two lobes, LB1 and LB2, are referred to as "Venus flytrap domains" (VFTs), since the GB1 VFT can "trap" ligands in its orthosteric binding site, located between the two lobes. Each VFT is connected to a canonical TMD via a stalk domain (Fig. 2A). This stalk consists of a relatively rigid, twisted three-stranded β sheet, formed by the linker connecting the VFT and TMD together with the long extracellular loop 2 (ECL2) of the TMD. A patch of charged residues provides additional stabilization between the stalk and the VFT (Fig. 3B). The stalk domain is unique to $GABA_B$, while all other class C receptors have a cysteine-rich domain as a connection between their extracellular and TMDs (Fig. 2B).

The GB1a isoform contains two N-terminal sushi domains, SD1 and SD2, with sequences homologous to complement control protein (CCP) domains, also known as short consensus repeats, which are present in the regulator of complement activation protein family (*46*). Although each of the sushi domains forms two intact disulfide bonds, only SD2 adopts a compact fold, while SD1 appears to be natively disordered (*39*). SD1 has been found, however, essential for binding to extracellular matrix and APPs. Structures of intact SD2 and of SD1 in complex with a 9-mer peptide derived from APP were solved by NMR (*39*, *40*). Both structures adopt a similar fold [root mean square distance (RMSD) = 2.1 Å] consisting of a small β sheet, connected by ordered loops.

The structure of the C-terminal CC domain shared between GB1 and GB2 was determined by x-ray crystallography (*20*). The CC resembles a classic "knobs-into-holes" motif with an extensive network of intersubunit hydrogen bonds. This crystal structure gave insights into the heterodimerization of the two subunits and revealed that the di-leucine ER retention signal is buried within the interface, facilitating trafficking of the GB1-GB2 heterodimer to the cell surface (*20*). The active state $GABA_B$ structure of Shaye *et al.* (*22*) showed an elongated density protruding from the intracellular side of GB2 at a 20° angle relative to the membrane surface, which was tentatively assigned to the CC domain. However, the local resolution was not sufficient for unambiguous building and inclusion of this domain in the final model. This observation could hint at a possibility that, besides trafficking, the CC domain could also play a

Table 1. Summary of available $GABA_B$ structures and details of structure determination methods. CHS, cholesteryl hemisuccinate; GDN, glyco-diosgenin; GFP, green fluorescent protein; LMNG, lauryl maltose neopentyl glycol.

Reference	PDB ID	Assembly	Resolution (Å)	Ligand(s)	Purification	Cell line	Detergent
Cryo-EM							
Shaye *et al.* (*22*)	6VJM	GB1-GB2	4.0	*apo*	Anti-Flag M2	Sf9	Digitonin
	6UOA		6.3	$SKF97541_{AGO}$	Anti-GFP NB		
	6UO9		4.8	$SKF97541_{AGO}$	Superose 6 Increase		
	6UO8		3.6	$SKF97541_{AGO}$ + $GS39783_{PAM}$			
Papasergi-Scott *et al.* (*24*)	6W2X	GB1-GB2	3.6	$CGP55845_{ANT}$	Anti-Flag G1	Sf9	GDN/CHS
	6W2Y	GB1-GB1	3.2	$CGP55845_{ANT}$	Ni-NTA		
					Superose 6		
Park *et al.* (*23*)	6WIV	GB1-GB2	3.3	*apo*	Anti-Flag M2	HEK293 $GnTI^-$	LMNG/CHS
					Mono Q		
					Superose 6		
Mao *et al.* (*25*)	7C7S	GB1-GB2	3.0	$CGP54626_{ANT}$	Ni-NTA	HEK293F	LMNG/CHS
					Anti-Flag M1		
	7C7Q	GB1-GB2 + G_i + scFv16	2.8	$Baclofen_{AGO}$ + $rac\text{-}BHFF_{PAM}$	Superose 6 Increase		
Kim *et al.* (*26*)	7CA5	GB1-GB2	7.6	*apo*	Anti-Flag G16	HEK293 $GnTI^-$	GDN/CHS/OG
					Anti-GFP DARPin		
	7CA3		4.5	$GABA_{AGO}$ + $rac\text{-}BHFF_{PAM}$	Anti-GST		
	7CUM		3.5	$CGP54626_{ANT}$ + $CLH304a_{NAM}$	Superose 6		
X-ray crystallography							
Geng *et al.* (*35*)	4F11	GB2 VFT	2.4		Anti-Flag M2	Sf9	
	4F12		3.0		Superdex 200		
Geng *et al.* (*36*)	4MQE	GB1-GB2 VFT	2.35	*apo*	Anti-Flag M2	Sf9	
	4MS4		1.90	$Baclofen_{AGO}$			
	4MS3		2.50	$GABA_{AGO}$			
	4MR7		2.15	$CGP54626_{ANT}$	Superdex 200		
	4MS1		2.25	$CGP46381_{ANT}$			
	4MR8		2.15	$CGP35348_{ANT}$			
	4MR9		2.35	$SCH50911_{ANT}$			
	4MQF		2.22	$Saclofen_{ANT}$			
	4MRM		2.86	$Phaclofen_{ANT}$			
Burmakina *et al.* (*20*)	4PAS	GB1-GB2 coiled coil	1.62		TALON	BL21 (DE3)	
					Mono Q		
					Superdex 75		
Zheng *et al.* (*37*)	6M8R	KCTD16 + GB2 C terminus	3.2		Ni-NTA	BL21 (DE3)	
					Q Sepharose		
					Superdex S200		
Zuo *et al.* (*38*)	6OCP	KCTD16 + GB2 C terminus	2.35		Co^{2+} IMAC	BL21-CodonPlus (DE3)-RIL	
					Superdex 200		
					Mono Q		

continue on next page

Reference	PDB ID	Assembly	Resolution (Å)	Ligand(s)	Purification	Cell line	Detergent
NMR							
Rice *et al.* (*40*)	6HKC	SD1 + APP 9mer			Ni-Sepharose Sephacryl S100	BL21 (DE3)	
Blein *et al.* (*39*)	1SS2	SD2			Mono S RP2	*Pichia pastoris*	

regulatory role in receptor signaling, which could warrant further investigations.

The orthosteric ligand-binding site is located at the interface between LB1 and LB2 of GB1 (Fig. 4). On the basis of the available x-ray and cryo-EM structures, both agonists and antagonists are anchored by several polar residues—such as S247, S248, S270, H287, E466—and a key aromatic residue W182 of LB1. Binding of an agonist leads to the closure of these two lobes by engaging two bulky aromatic LB2 residues, Y367 and W395, sandwiching the ligand.

Park *et al.* (*23*) and Papasergi-Scott *et al.* (*24*) both described putative calcium binding to the LB2 lobe of GB1, in close proximity to the orthosteric binding site of $GABA_B$ (Fig. 3A). While recent structures of receptors across different GPCR classes have started to hint at a broader role of ions in ligand binding and receptor modulation (*47*, *48*), notably, calcium was not identified in the previous high-resolution crystal structures of $GABA_B$ VFT (*36*), where water molecules were modeled at corresponding sites. In the past, several studies reported a positively modulating effect of a broad range of divalent cations on $GABA_B$ (*49*–*51*), while Park *et al.* (*23*) have revealed the ion identity using mass spectrometry. The positive modulation could be explained by a stabilizing effect of the ion on the conformation of the loop containing W395, which is one of the key residues in LB2 that interacts with both agonists and antagonists (Fig. 4, C to F).

Unexpectedly, several groups (*23*–*26*) also identified endogenous phospholipid binding sites, located within both TMDs of the heterodimer (Fig. 3, C and D). Phospholipid binding has been suggested to confer a positive effect on receptor stability and integrity, as well as to modulate signaling. The locations of these sites within $GABA_B$ TMDs correspond to orthosteric ligand-binding sites in class A and B GPCRs and allosteric sites in class C and F receptors; however, no double-chain phospholipid binding in those pockets has been previously observed. The identity of these lipids was probed by mass spectrometry and assigned as PE (phosphatidylethanolamine) 38:5 (GB1) and PC (phosphatidylcholine) 38:2 (GB2) (*23*). The overall binding mode of the endogenous phospholipids appears to be conserved between the two subunits, with an intricate network of interactions with most TM helices, except for TM1 and TM4, forming a large interface contact area of ~1000 $Å^2$. The head group of each lipid is anchored through polar interactions with conserved $R^{3.32}$ in TM3 and histidine in ECL2 (H760 in GB1 and H647 in GB2), as well as with R714 in ECL3 of GB2. The port of lipid entry into the TMD is most likely located between TM5 and TM6, as one of the acyl tails protrudes through a gap between these two helices in both subunits. Mutational studies suggested that PC 38:2 acts as a negative allosteric modulator (NAM), as it appears to stabilize the inactive state of $GABA_B$ (*24*); however, further studies are required to fully understand the biological function of these interactions.

INACTIVE STATE OF $GABA_B$

All five cryo-EM publications (*22*–*26*) present the receptor in an inactive state (three *apo*- and three antagonist-bound structures, Table 1). Their VFTs are very similar within an $RMSD_{VFT}$ of ~0.8 to 1.2 Å and align equally well with the previously published x-ray structures of *apo*- and antagonist-bound states of the VTFs (*36*). Antagonists, CGP54626 and CGP55845, are anchored in the orthosteric site of GB1 VFT by polar interactions with LB1 residues S247, S270, H287, E466, similarly to agonists; however, they have bulky substituents at both amino and phosphinic acid ends interacting with Y367 and W395 from LB2 in its open conformation (Fig. 4, E and F). This observation could hint toward the mechanism of these antagonists acting like a "doorstop," preventing the VFT from closing for activation, which is consistent with their function as inverse agonists in constitutively active receptor mutants (*52*). Kim *et al.* (*26*) used a NAM CLH304a along with the antagonist CGP54626 for obtaining their structure [Protein Data Bank (PDB) ID 7CUM]; however, no density for the NAM was observed. The TMD conformations between the six structures are very similar ($RMSD_{TMD}$ ~ 1.1 to 1.4 Å), all showing a heterodimer interface with the proposed intersubunit latch at the intracellular tips of TM5 and TM3, consisting of $H689^{3.55}$, $E790^{5.60}$ in GB1 and $H579^{3.55}$, $E677^{5.60}$ in GB2, which locks the receptor in its inactive state (Fig. 3E). Notably, Park *et al.* (*23*) and Kim *et al.* (*26*) described an extensive network of cholesterol molecules surrounding this exact interface, potentially stabilizing the intersubunit latch. In addition, in both subunits, the intracellular ends of TM3 and TM6 are constrained by an ionic lock between $K^{3.50}$ and $D^{6.35}$, which is conserved in class C GPCRs (*53*).

Comparing the inactive state structures overall, the most pronounced differences are found in the relative orientation of the VFTs with respect to the TMDs, of which all five are captured in a slightly different relative angle (within 2°), with no apparent correlation between *apo*- and antagonist-bound states, in line with Shaye *et al.*'s (*22*) molecular dynamics (MD) simulations that proposed some freedom of motion of the VFT relative to the TMD in the inactive state. As a caveat, this relative motion could also be explained by the fact that all above mentioned data processing schemes either involved separate treatment of the VFT and TMDs, and subsequent merge of the individually refined maps, or used local refinement strategies, allowing for a flexible hinge between the two domains, to obtain high-resolution reconstructions.

$GABA_B$ ACTIVE STATE

Three of the five studies (*22*, *25*, *26*) were able to obtain a high-resolution reconstruction of the active state of $GABA_B$. In all three structures, a PAM was required in addition to an agonist to lock the

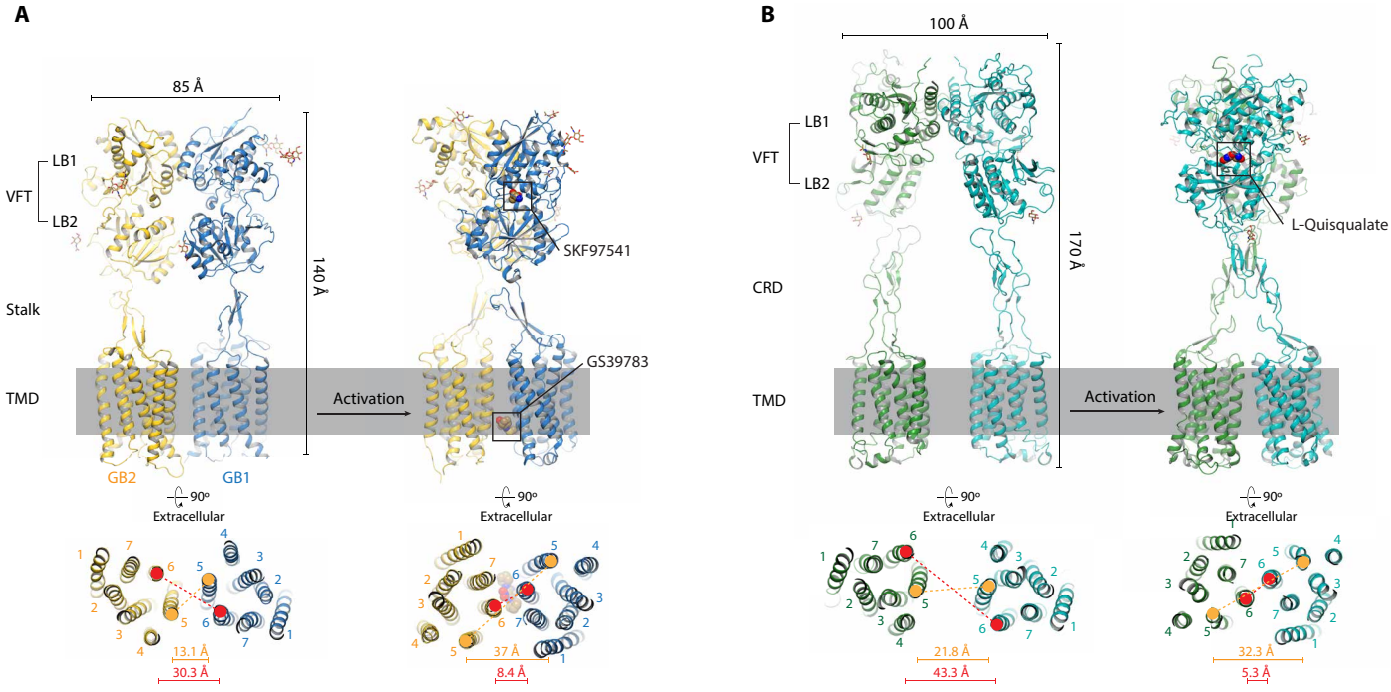

Fig. 2. Comparison of $GABA_B$ structure and activation with mGluR5. (**A**) Structures of $GABA_B$ in *apo* inactive [Protein Data Bank (PDB) ID 6VJM, left] and agonist-bound active (6UO8, right) states are shown in side views (top) and looking on TMDs from the extracellular side (bottom). (**B**) Similar views as in (A) for mGluR5 receptor in *apo* inactive (6N52, left) and agonist-bound active (6N51, right) states. Membrane boundaries are shown as a gray slab. $GABA_B$ is the only member of class C GPCRs lacking the cysteine-rich domain (CRD); instead, its elongated ECL2 forms a three-stranded β sheet together with a linker connecting VFT and TMD, termed stalk. A common mechanism of activation in class C GPCRs involves a twisting motion of each subunit along the (pseudo-)symmetry axis in which TM5s move apart while TM6s approach closer forming the (hetero-)dimeric interface. The distances shown in lower panels are measured between Cα atoms of residues 5.41 in TM5 and 6.56 in TM6. GB1, GB2, and two mGluR5 subunits are colored in blue, gold, and green/teal, respectively.

receptor in the active state. One of the three structures (PDB ID 7C7Q) was captured in a complex with a G_i protein (*25*), although the local resolution around the G_i protein was reported to be much lower than the rest of the receptor, precluding modeling of the G_i protein itself. In the active state, the VFTs adopt closed(GB1)-open(GB2) conformation upon agonist binding, while the TMDs rearrange to get into close contact along a TM6-TM6 interface, which includes mostly hydrophobic interactions, except for two hydrogen bonds (GB1-Y810$^{6.44}$ with GB2-N698$^{6.45}$ and GB1-N811$^{6.45}$ with GB2-Y697$^{6.44}$). The ionic lock between TM3 and TM6 in GB2 is broken, and the intracellular ends of TM3, TM4, and TM5 are shifted by 4 to 6 Å with respect to their positions in the inactive state, opening up a cleft on the intracellular side of GB2 for G protein binding. All three structures are similar (RMSD < 2 Å), showing overall rearrangements required for the activation of $GABA_B$ while indicating that two structurally different PAMs are binding to the same allosteric site at the heterodimer TMD interface. However, comparing these three structures, the Shaye *et al.* (*22*) structure (PDB ID 6UO8) appears slightly bulkier overall—based both on the longer distance between the VFT lobes (~ 2.5 Å, measured between Cα atoms of GB1-Q577 and GB2-K467) and on a slightly looser packing of the TMDs (~ 2 Å longer TM5-TM5 distance, measured between Cα atoms of GB1-Y774$^{5.44}$ and GB2-Y661$^{5.44}$). In summary, this suggests that the active state conformation of $GABA_B$ may slightly differ depending on the specific combination of an agonist and PAM; however, it does not seem to depend on the presence of a G protein.

PAM BINDING SITES COMPARISON

One of the most notable discoveries in the reported cryo-EM structures was the identification of the PAM binding sites at the interface of the two TMDs in the active state of $GABA_B$. Notably, two chemically distinct PAMs, GS39783 (6UO8) and (+)-BHFF (7C7Q and 7CA3), were found to bind at overlapping sites, buried inside the membrane and composed of residues from TM5, TM6, and TM7 of both subunits (Fig. 4) (*22*, *25*, *26*). Both PAMs have amphiphilic properties, allowing them to partition into and penetrate through the membrane. Mao *et al.* (*25*) and Kim *et al.* (*26*) used rac-BHFF as PAM but found that the (+)-BHFF enantiomer fits better in the experimental density, in agreement with pharmacological data (*54*). (+)-BHFF occupies a predominantly hydrophobic pocket made of residues GB1-A788$^{5.58}$, GB1-Y789$^{5.59}$, GB1-M807$^{6.41}$, GB1-Y810$^{6.44}$, GB2-K690, GB2-Y691, and GB2-M694$^{6.41}$, and it forms one hydrogen bond with GB1-K792^{ICL3}. On the other hand, GS39783 is anchored by a hydrogen bond with GB2-N698$^{6.45}$ and a stacking interaction with GB1-Y810$^{6.44}$, as well as by extensive hydrophobic and polar interactions with GB1-Y789$^{5.59}$, GB1-K792^{ICL3}, GB1-M807$^{6.41}$, GB2-M694$^{6.41}$, and GB2-Y697$^{6.44}$.

G PROTEIN BINDING

Mao *et al.*'s study (*25*) is the only one of the five studies that describes a structure of $GABA_B$ in complex with a G_i protein. Initially, the authors tried capturing the structure of the complex using a

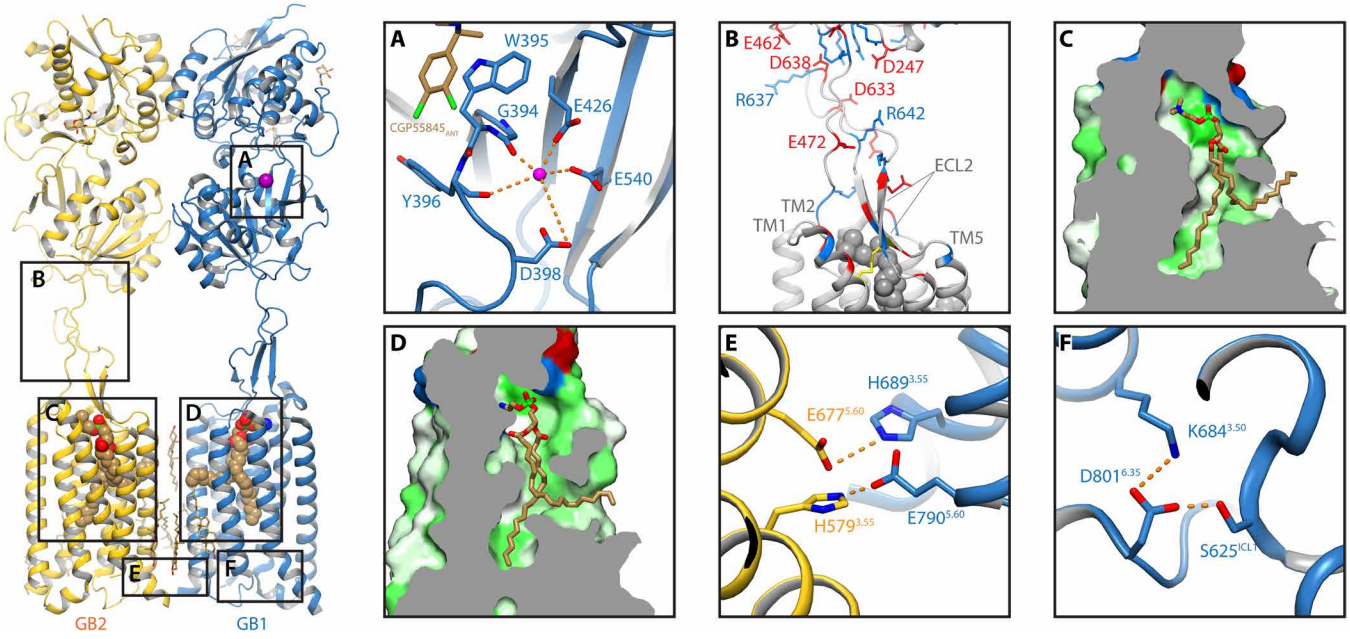

Fig. 3. Structural features of $GABA_B$. Left: Overall view of *apo* $GABA_B$ in the inactive conformation (PDB ID 6WIV). (**A**) Representative model of Ca^{2+}-binding site in GB1 bound to antagonist CGP55845 (6W2V). (**B**) In each subunit, VFT is connected to TMD via a stalk domain that is stabilized by a network of electrostatic interactions between positively (blue) and negatively (red) charged residues. (**C** and **D**) Binding sites for endogenous phospholipids: PC 38:2 in GB2 TMD (C) and PE 38:5 in GB1 TMD (D). Receptor surface is colored by hydrophobicity (*125*), where more hydrophobic residues are shown in darker shade of green and charged residues are colored using the same color scheme as in (B). (**E**) Intersubunit lock between TM3 and TM5 at the heterodimeric interface stabilizes inactive conformation. (**F**) Activation-related ionic lock between TM3 and TM6 in GB1 TMD. Ligand and lipid molecules are shown as sticks with carbon atoms colored in sand, oxygen in red, nitrogen in blue, chlorine (A) and phosphor (C and D) in light green, sulfur in yellow, and calcium ion in magenta. GB1 and GB2 subunits are colored in blue and gold, respectively.

full-length $GABA_B$, which resulted in sample aggregation. Removing the CC increased the yield of the receptor and facilitated the formation of $GABA_B$-G_i complex. To assemble the complex, HEK293F cells expressing truncated $GABA_B$-ΔCC construct were combined with Sf9 cells expressing G_{i1} protein, followed by addition of an agonist baclofen, a PAM rac-BHFF, an apyrase to hydrolyze guanosine 5′-triphosphate, and a G_i protein–stabilizing antibody scFv16. Purified complex was used to collect single-particle cryo-EM data, revealing three distinct major conformations identified by 3D classification. Further refinement produced three reconstructions that differed only by the binding position of the G_{i1} protein: (i) 17% of particles were found in a state termed B1 (8.8-Å resolution) in which G_{i1} is bound to GB1, (ii) 74% of particles were found in a B2a state (6.8 Å) in which G_{i1} is bound to GB2, and (iii) 9% of particles were found in a B2b state (8.6 Å) in which G_{i1} is also bound to GB2 but in a different orientation from the B2a state (*25*). This distribution agrees with the asymmetric model of $GABA_B$ signaling in which G protein couples predominantly to GB2. Although it was not possible to model the G_{i1} protein unambiguously, its $G_{\alpha i}$ subunit appears to be in an activated nucleotide-free form based on the separated densities for the α-helical (AHD) and Ras-like domains. Compared to class A GPCRs, the opened upon activation cleft on the intracellular side of GB2 is very shallow, preventing the C-terminal α5 helix of $G_{\alpha i}$ from the insertion in the GB2 TMD. This leads to a much smaller G_{i1} protein–binding interface in which the α5 helix interacts mostly with intracellular loops and the tip of TM3, resulting in a more flexible binding of G_{i1} that allows multiple conformations, where the B2a state is the most stable, while the B2b state in which G_{i1} is rotated about 90° may represent an intermediate state.

GB1 HOMODIMER

While the primary signaling unit of $GABA_B$ is a heterodimer, it has been shown that each subunit can form homodimers (*55*) and that the two subunits can assemble into higher-order oligomers (*56*). Papasergi-Scott *et al.* (*24*) observed that, along with the GB1-GB2 heterodimer, they could purify a GB1 homodimer. Subsequently, they collected cryo-EM data for a GB1 homodimer bound to an antagonist CGP55845, which resulted in a 3.2-Å resolution structure (PDB ID 6W2Y) with each subunit occupied by the antagonist and arranged in a twofold symmetry (*24*). In the antagonist-bound homodimer, the VFTs of each subunit adopt a fully open conformation, very similar to the GB1 subunit of the antagonist-bound x-ray structure (4MR7, RMSD = 0.86 Å), locked in an inactive conformation (*36*). The overall conformation of the homodimer, however, is similar to the conformation of the active state heterodimer in which the LB2 lobes of both subunits come in contact, rearranging the TMDs to interact along TM6. Despite resembling the active-like subunit arrangement, there are no conformational changes within TMDs, and the homodimer is unable to bind to G protein and other transducers.

ACTIVATION MECHANISM OF $GABA_B$

In addition to two major stable receptor conformations, active and inactive, Shaye *et al.* (*22*) observed two distinct intermediate states (int-1 and int-2) along the receptor activation trajectory in the presence of an agonist (Fig. 5). Both intermediate states have comparatively lower resolution (6.3 and 4.8 Å), as they are likely present in a dynamic equilibrium, preventing assignment of most amino acids. These

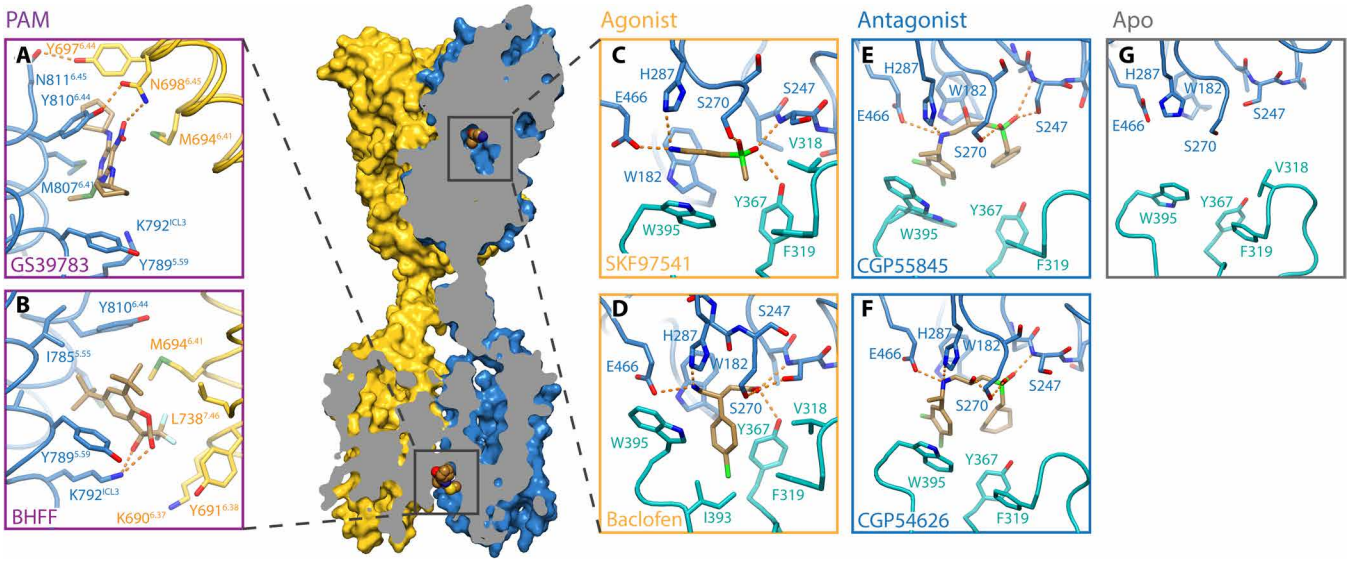

Fig. 4. Structural details of orthosteric ligands and PAM binding to $GABA_B$. (**A** and **B**) Binding of PAMs at the heterodimeric TMD interface: GS39783 (PDB ID 6UO8) (A) and (+)-BHFF (7C7Q) (B). (**C** and **D**) Binding of agonists in the orthosteric site of GB1 VFT: SKF97541 (6UO8) (C) and baclofen (7C7Q) (D). (**E** and **F**) Binding of antagonists in the orthosteric site of GB1VFT: CGP55845 (6W2X) (E) and CGP54626 (7C7S) (F). (**G**) Orthosteric ligand-binding site of GB1 VFT in the *apo* state (6VJM). Ligands are shown as sticks with carbon atoms colored in sand, oxygen in red, nitrogen in blue, chlorine and phosphor in light green, sulfur in dark green, and fluorine in pale blue. GB1 and GB2 subunits are colored in blue and gold, respectively. In (C) to (G), LB1 and LB2 of GB1 subunit are colored in blue and teal, respectively.

intermediate state structures, nevertheless, provide important insights into the activation pathway of $GABA_B$. They add crucial details to the large conformational rearrangements that delineate the activation pathway, where, first, the LB lobes of the GB1-VFT close upon agonist binding (int-1 state), likely accompanied by breaking the intersubunit latch between the two TM5s. After the closure of the VFT, a rearrangement of the entire heterodimer interface is observed, which closes the gap between the LB2 domains of the two VFTs while forming a new TMD interface along TM6s (int-2 state).

The presence of these intermediate states highlights that $GABA_B$ activation is decoupled into at least two main transitions, as opposed to a single concerted motion. The second intermediate state—in contrast to the final active state structures—also demonstrates that the GB2 TMD remains in the inactive conformation, with the TM6-TM3 ionic lock still intact. Only the addition of a PAM that stabilized this state for structure determination allowed capturing the final step of the activation-related rearrangements, namely, straightening and displacements of intracellular parts of TM3 to TM5, which open a cleft that accommodates G protein binding. These findings have general implications for our understanding of $GABA_B$, as they showcase a tightly regulated activation mechanism with multiple activation barriers, which have to be overcome in order for the receptor to reach its fully active, signaling state. Compared to other homodimeric class C receptors [reviewed in (*57*)], the activation mechanism of $GABA_B$ is unique in that it is an entirely asymmetrical process, although ultimately resulting in a similar TMD interface along TM6 (Fig. 2). The discovery of the intermediate states in $GABA_B$ activation is in agreement with submillisecond fluorescence resonance energy transfer studies of mGluR1, which also proposed two intermediate states along its activation pathway (*58*). Additional insights in the asymmetric activation mechanism have been provided by spectroscopic studies of mGluR heterodimers (*59*) and $GABA_B$ receptors (*60*).

Comparing the conserved motifs in class A and C receptors in more detail, notable similarities and differences that can be attributed to their different modes of action become apparent. (i) The ionic lock between $K^{3.50}$ and $E/D^{6.35}$, conserved in class C receptors, is also observed in the inactive state in both $GABA_B$ subunits (*61*). A similar conserved lock is present in class A GPCRs between the residues $R^{3.50}$ and $D/E^{6.30}$, where mutational disruptions of the lock showed increased basal activity (*62*, *63*). It should be noted in this context that generic residue numbering differs between GPCR classes and depends on the intraclass conservation of a residue rather than its absolute position relative to the lipid bilayer (*64*). The ionic lock appears to play an important role in $GABA_B$ signaling, since it is broken in GB2 in the active state, and mutating GB2-$K^{3.50}$ to an acidic residue results in a complete loss of function (*63*). (ii) The $FxP^{7.50}KxY$ motif at the intracellular end of TM7 is highly conserved in class C GPCRs and shares similarity with the $NP^{7.50}xxY$ motif of class A. In class A, $Y^{7.53}$ plays a critical role in stabilizing the TM3-TM7 interface in the active state. However, in class C, $Y^{7.53}$ (mGluR) or $R/I^{7.53}$ (GB1/2) faces toward the outside of the helical bundle and does not make any contacts with TM6. On the other hand, $K^{7.51}$ participates in a network of hydrogen bonds with the ionic lock through $N^{2.39}$, $S625^{ICL1}$ in GB1 and $S515^{ICL1}$ in GB2, thereby stabilizing the intracellular segment of the TMD. (iii) The residue $W^{6.48}$ from the highly conserved $FxxCWxP^{6.50}$ motif in class A GPCRs was proposed to act as a "toggle switch," changing its conformation upon activation (*65*). In addition, $F^{6.44}$ belongs to the P-I-F motif that rearranges upon agonist binding (*66*), initiating a cascade of conformational changes that result in the large-scale movements of TM5 and TM6, and enables the receptor to engage with G protein. The mGlu receptors, on the other hand, feature a highly conserved $W^{6.50}$ residue at the equivalent position; however, in mGluR, it holds a different conformation, forming a bridge between TM5 and TM6 (*53*). In both GB1 and GB2 of $GABA_B$, this residue is replaced with a Cys residue to

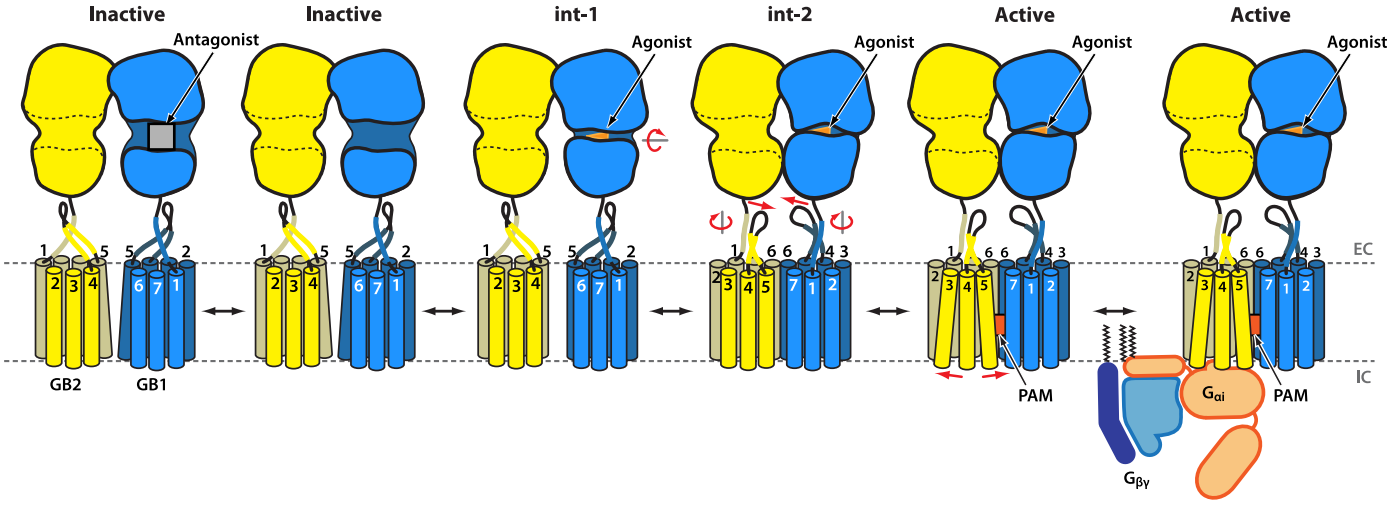

Fig. 5. Schematic mechanism of $GABA_B$ inhibition and activation. In the *apo* state, the receptor adopts an inactive conformation with both VFTs being open and TMDs contacting each other on the intracellular side via an intersubunit lock between TM3 and TM5. Antagonist binding prevents GB1 VFT from closing and keeps the receptor in the inactive state. Agonist binding triggers the series of transitions, first, closing GB1 VFT and releasing the intersubunit lock (int-1 state) and, then, bringing LB2 lobes of two VFTs in contact, which, in turn, induces TMD rearrangement placing them in contact via TM6 (int-2 state). Last, PAM binding at the TM6 interface of two TMDs stabilizes this interface, leading to TM3, TM4, and TM5 to straighten and shift on the intracellular side of GB2, opening a shallow cleft for G protein binding (active state). Schematic pictures of $GABA_B$ conformational states are aligned by their VFTs. EC, extracellular side; IC, intracellular side.

avoid the steric clash with the phospholipid occupying the TMDs and allows the hydrophobic chain of the lipid to enter a cavity created at the interface of TM5 and TM6 of both subunits.

IMPLICATIONS OF $GABA_B$ STRUCTURES FOR UNDERSTANDING DISEASE AND DRUG DISCOVERY

Mutational model of $GABA_B$ and its correlation to different diseases

$GABA_B$ is considered the oldest member of class C GPCRs (*67*). Given the importance of GABA as a major inhibitory neurotransmitter in the brain, it is perhaps expected that the amino acid sequence of $GABA_B$ receptor is evolutionarily constrained. This results in an exceptionally low number of naturally occurring variants: Among the 19,704 human Ensembl transcripts in the gnomAD (v 2.1.1) database of naturally occurring sequence variants in more than 15,000 genomes and more than 125,000 exomes (*68*, *69*), GB1 and GB2 both rank in the 99th percentile (127th/151st, respectively) and first and second among 697 GPCRs mapping to human transcripts, in terms of the lowest observed number of missense mutations (i.e., nucleotide changes leading to an amino acid substitution), normalized for gene length and sequence context (*70*, *71*). In particular, both subunits display fewer than half (ratios of 0.42 and 0.44, respectively) of the number of expected missense mutations, i.e., are strongly intolerant of (such) variations.

We limit the following analysis of variants to missense mutations, since their effect can be most immediately rationalized based on the experimental $GABA_B$ structures that have now become available. When mapping the location of the observed variants onto these structures, it becomes apparent that they are underrepresented in areas associated with protein function and ligand binding, as described above. For example, there are no missense mutations within the orthosteric ligand-binding site or ion-coordinating residues of GB1, the ionic lock is unaffected, as well as the intersubunit latch and the FxPKxY motif in both subunits. A single missense mutation has been observed for a residue linking the ionic lock and the FxPKxY motif (GB2-N520$^{2.39}$T); two missense mutations in the nonpolar interaction interface between TM5s that is associated with the inactive receptor state (GB1-L779$^{5.49}$V and GB2-L669$^{5.52}$S); and a small number of missense mutations near the PAM binding site between the intracellular tips of TM5 and TM6 (GB1-A788$^{5.58}$S, T791$^{5.61}$N, R803$^{6.37}$Q/P, and G806$^{6.40}$V). A number of variants slightly higher than that observed for microswitches map to residues in the proximity of the two endogenous phospholipids, most of which preserving the hydrophobic character of this region.

While mapping these mutations to motifs of known or presumed function in $GABA_B$ and other GPCRs earmarks them for more detailed molecular studies, several missense mutations in $GABA_B$ have already been reported to have strong association to disease, particularly the Rett syndrome and epileptic encephalopathy (*72*–*74*). Mapping the most notable variants—such as GB2-A567$^{3.43}$T, GB2-G693$^{6.40}$W, GB2-S695$^{6.42}$I, GB2-I705$^{6.52}$N, and GB2-A707$^{6.54}$T—onto the available $GABA_B$ structures revealed their distribution across the GB2 TMD. In particular, GB2-A567$^{3.43}$T is situated at the bottom of the lipid-binding crevice of GB2 and has been found to impair receptor signaling efficacy (*73*). Of the other residues, GB2-I705$^{6.52}$N points toward the lipid bilayer, which could potentially destabilize the TMD and affect TM6-TM6 dimerization, while GB2-A707$^{6.54}$T is close to the opening through which the lipid enters the pocket. Residues GB2-G693$^{6.40}$W and GB2-S695$^{6.42}$I are at the interface of TM6 with TM5 and TM7, respectively, close to the allosteric binding site.

Pharmacological modulation of the $GABA_B$ receptor

While benzodiazepines are widely used as stereotypical modulators of $GABA_A$ receptors with sedative, hypnotic, anticonvulsant, and

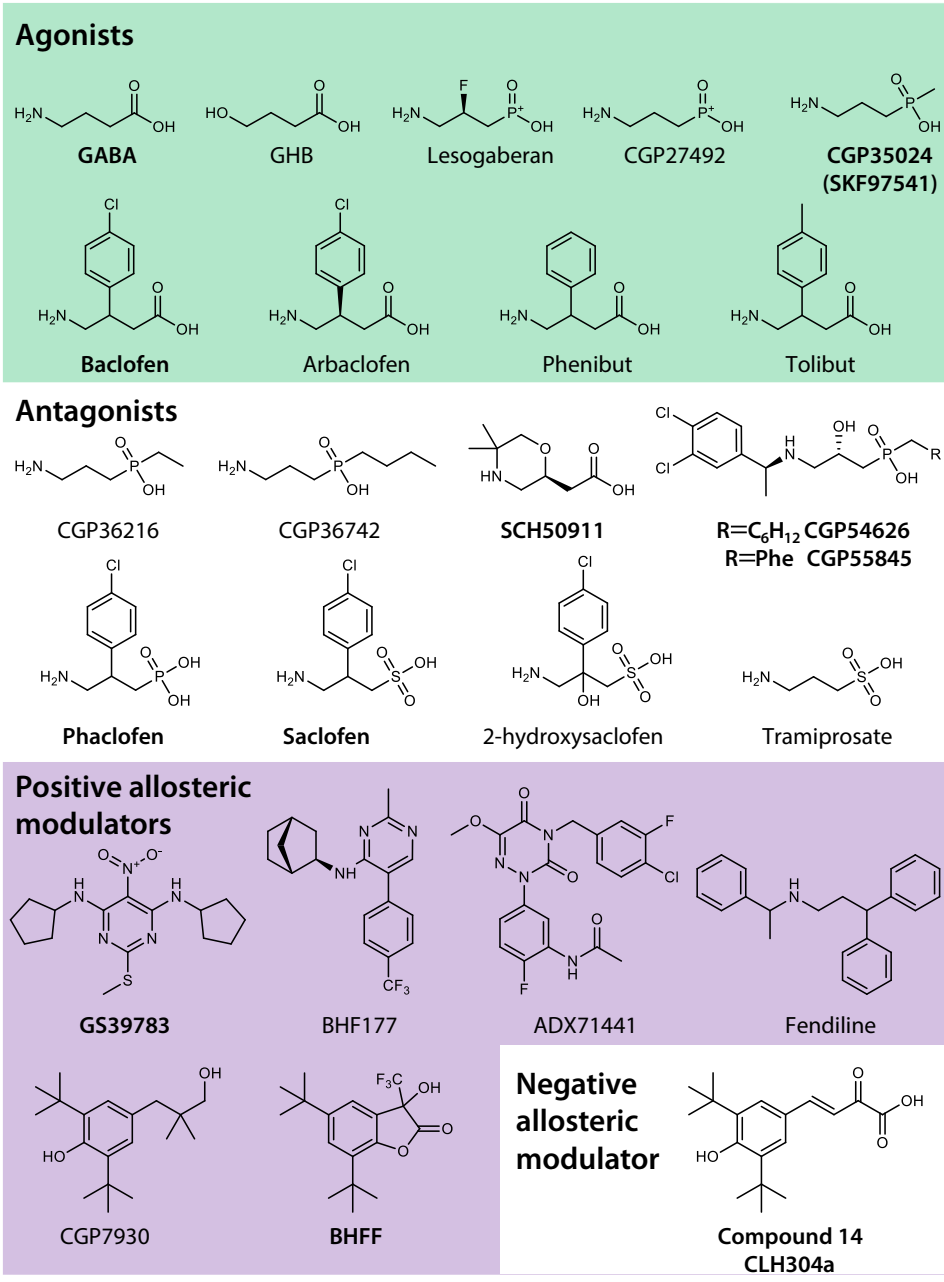

Fig. 6. Chemical structures of select $GABA_B$ ligands. Compounds used for structural studies described in this review are highlighted in bold, and, in the following, ChEMBL (*126*) identifiers or PubChem (*127*) identifiers are given where available. Clinical trial identifiers (clinicaltrials.gov) and indications are listed where available. Agonists: GABA (CHEMBL96), GHB (γ-hydroxybutyric acid; CHEMBL1342, approved for cataplexy, NDA 021196), Lesogaberan (CHEMBL448343, phase 2 clinical trial for gastroesophageal reflux disease, NCT01043185), CGP27492 (CHEMBL112203), CGP35024 (CHEMBL112710), baclofen (CHEMBL701, approved antispasmotic and muscle relaxant, NDA 017851), arbaclofen (CHEMBL301742) (phase 3 clinical trials for autism spectrum disorder and fragile X syndrome, NCT01282268 and NCT01706523), phenibut (CHEMBL315818, approved in Russia), and tolibut (PubChem ID 49344). Antagonists: CGP36216 (CHEMBL325921), GCP36742 (CHEMBL112797, phase 2 clinical trials for Alzheimer's disease, NCT00093951), SCH50911 (CHEMBL1895916), CGP54626 (CHEMBL1213187), CGP55845 (CHEMBL455185), phaclofen (CHEMBL1255941), saclofen (CHEMBL312403), 2-hydroxysaclofen (CHEMBL1256573), and tramiprosate (CHEMBL149082, phase 3 clinical trials for Alzheimer's disease, NCT00088673). PAMs: GS39783 (CHEMBL392394), BHF177 (CHEMBL2346820), ADX71441, fendiline, CGP7930 (CHEMBL1256697), and BHFF (CHEMBL2322946). Negative allosteric modulator: compound 14 (CHEMBL3326377).

muscle relaxant properties, fewer approved drugs target $GABA_B$ (*75*–*77*). We will give a brief overview of compounds targeting $GABA_B$ described to date, spanning a variety of pharmacological efficacies including orthosteric agonists and antagonists, as well as positive and NAMs (Fig. 6), and highlight their clinical application.

The inability of the endogenous agonist, GABA (in structures with PDB IDs 4MS3 and 7CA3), and its derivatives to efficiently penetrate the blood-brain barrier (BBB) (*78*) has motivated the development of baclofen (*79*, *80*) (in 4MS4 and 7C7Q), which has been approved as a muscle relaxant and antispasmodic agent in the United

States in 1977. The subsequent identification of its bioactive enantiomer R-(−)-baclofen (arbaclofen) (*81*, *82*) and its binding selectivity profile has helped to uncover the existence of a distinct subset of GABA binding sites and the $GABA_B$ receptor subtype a few years later (*32*). Since baclofen requires active transport across the BBB (*83*), attempts to target $GABA_B$ in the CNS prompted the development of more readily bioavailable formulations and prodrugs (*84*–*89*). γ-Hydroxybutyric acid (GHB), which is metabolized into GABA and itself acts as a weak agonist of $GABA_B$ (*90*, *91*), displays anesthetic and intoxicating properties and is thought to elicit its effects through a mechanism involving an additional receptor (*79*, *90*, *92*, *93*). Approved for treatment of cataplexy and narcolepsy (*91*, *94*, *95*), GHB and its salts are controlled substances notorious for their illegal and recreational use. While BBB penetration is required for CNS action, a different strategy is used for targeting peripheral $GABA_B$ receptors. Thus, Lesogaberan, an agonist with poor brain penetration to avoid CNS side effects, has reached phase 2 clinical trials for the treatment of gastroesophageal reflux disease where it failed to show significant efficacy, halting its further development (*96*).

To date, no $GABA_B$ receptor antagonist has found clinical approval, although they are promising agents for mediating antidepressant (*97*), behavioral, and neuroprotective effects (*98*). Functionally, antagonizing the inhibition of GABA-mediated neurotransmitter release such as glutamate, noradrenaline, or serotonin could enhance their function, thereby indirectly modulating their downstream effectors. The first selective antagonists described were phaclofen (in 4MRM), saclofen (in 4MQF), and 2-hydroxysaclofen (*99*–*101*) Notably, extensions of the methyl moiety of the agonist CGP35024 (SKF97541, in 6UO8, 6UO9, and 6UOA) (*102*) were shown to confer antagonism [CGP36216 and CGP36742 (*103*, *104*)]. Antagonists CGP36742 and tramiprosate (homotaurine) have been investigated as treatments of Alzheimer's disease (*105*, *106*), with the latter still available as a dietary supplement in the United States, while the orally active SCH50911 (*107*) has been in preclinical development as a treatment for absence seizures. The low affinity of all of these antagonists limits their usefulness as tool compounds (*79*), prompting development of compounds with nanomolar affinity such as CGP54626 (*16*) (in 4MR7, 7C7S, and 7CUM) and the related CGP55845 (*108*) (in 6W2X and 6W2Y).

Improvement of ligand potency and selectivity as well as bioavailability remains an active topic of research that has motivated the exploration of a multitude of molecular decorations of the GABA scaffold. The high-resolution $GABA_B$ structures help to rationalize structure-activity relationship data for many of these compounds and better understand the functional consequence of the ligand pharmacophore on receptor function. GABA consists of a carboxylic acid and an amino group connected by a three-carbon aliphatic chain. Substitution of the amino group in GABA can decrease its potency or render the resultant molecules inactive; on the other hand, substituting the carboxylic acid group with a phosphinic acid (CGP27492) increased the agonist potency by 15 times (*109*, *110*), although it showed reduced activity for in vivo assays (*79*). Adding a methyl group to the phosphinic acid (SKF97541) enhanced an in vivo activity, demonstrating nociceptive responses at lower doses compared to baclofen and without any sedation effect (*111*). However, replacing the methyl group with bulkier ethyl or butyl converts the full agonist SKF97541 into a partial agonist CGP36216 or an antagonist CGP36742, respectively. We attribute this behavior to a two-step transition involved in VFT closure. Initially, an agonist binds to the LB1 of GB1 governed by a network of hydrogen bonds between the amino and carboxy (or phosphinic acid) groups of the ligand and residues in the binding pocket. The amino group interacts with E466 and H287 while the carboxylic or phosphinic group forms a network of hydrogen bonds with S270 and S247 (Fig. 4). In addition, the central aliphatic chain of the ligand makes van der Waals contacts with W182. Removing the amino or carboxy group of the ligands reduces polar interactions rendering it inactive and therefore unable to bind to GB1 VFT. The second step involves the closure of GB1 VFT that adds interactions with residues in the second lobe. These interactions are mainly hydrophobic or aromatic and are mediated by several residues such as W395, V318, and F319 in the LB2 that patches the ligand between the two lobes. In addition, Y367 stabilizes agonist binding by forming a hydrogen bond to ligand's carboxy/phosphinic acid end via its carbonyl group and making van der Waals interactions with the hydrophobic core of the ligand. Adding bulky groups to either end of the GABA scaffold or increasing the length of its aliphatic chain renders the ligand an antagonist by introducing steric clashes with Y367 and/or W395 and preventing the closure of LB2.

Allosteric modulators as novel opportunity for therapeutic intervention

Allosteric modulators promise safer alternatives to orthosteric synthetic ligands as they can modulate receptor signaling without replacing the action of endogenous ligands. PAMs have the ability to potentiate response to endogenous agonists while binding at distal sites (*108*). They have little to no intrinsic activity and open up chemical space and the possibility for specific receptor modulation without being constrained to the endogenous ligand chemotype. Their ability to fine-tune receptor response to endogenous agonists where physiologically relevant, and to potentiate effects of co-administered exogenous agonists, minimizes their abuse potential and makes them a sought-after class of compounds for clinical applications (*112*–*114*). In case of $GABA_B$ receptor, a number of PAMs have been identified (Fig. 6), with CGP7930 (*115*), followed by pyrimidine-based GS39783 (*116*) (in 6UO8), prototypical examples of PAMs that have found initial promise in animal models related to substance abuse, and showed anxiolytic effects, motivating their continued clinical development. The fluorinated benzofuranone derivative rac-BHFF (in 7C7Q and 7CA3) was obtained in the process of optimization of CGP7930. More recently, the CGP7930 scaffold has been modified to obtain the first NAM, compound 14 (*117*), also known as CLH304a. Its molecular similarity to the PAM CGP7930, juxtaposed with the disappearance of the well-defined PAM binding site formed by heteromeric contacts around the intersubunit latch region, warrants the future mechanistic exploration of NAMs.

CONCLUSIONS

Recent comprehensive cryo-EM studies described in this review have markedly furthered our understanding of the structure-function relationship of the metabotrobic $GABA_B$ receptor and shed new light on its complex biology and pharmacology. High-resolution structures of the near full-length receptor obtained in several conformational states provide detailed insights into the unique asymmetric activation mechanism of this heterodimeric receptor. Binding of an agonist in the GB1 VFT triggers a series of concerted motions leading

to conformational changes in GB2 TMD, priming it for interactions with and activation of G proteins. This activation mechanism is fundamentally different from that of class A, B, and F GPCRs in which the hallmark of activation involves large-scale shifts of TM5, TM6, and TM7 on the intracellular side, opening a large cleft for engagement of G proteins and β-arrestins. On the contrary, in $GABA_B$ and, likely, other class C receptors, the motion of TM6 in the active state is constrained by the hetero(or homo)-dimeric interface, while, instead, TM3, TM4, and TM5 of GB2 shift upon activation, creating a relatively shallow groove, mostly within intracellular loops, which could explain the high plasticity of $GABA_B$ interactions with G_i protein and difficulties in capturing the structure of such complexes. The activation transition of $GABA_B$ occurs in at least three discrete steps involving two intermediate states, and these states could help to analyze effects of specific mutations and potentially be targeted by NAMs. In addition to these mechanistic insights into receptor activation, new structures revealed previously unknown allosteric sites for calcium in GB1 VFT, endogenous phospholipids inside of both TMDs, and PAMs at the interface between two TMDs.

Besides the advances of our understanding of $GABA_B$, a list of important open questions regarding its structure and function remains. Although difficult to achieve, a high-resolution structure of a $GABA_B$-Gi complex would unveil a critical milestone, completing structural characterization of the receptor activation trajectory and helping to decipher G protein recognition, selectivity, and activation mechanisms. Along the same lines, structural identification of NAM binding sites would provide essential templates for structure-based design of novel therapeutic modulators.

In addition to G proteins and KCTDs, high-resolution proteomics identified more than 20 soluble and membrane proteins that interact with $GABA_B$ (*118*). It has been proposed, therefore, that $GABA_B$ functions within macromolecular signaling complexes with defined architecture but diverse composition, which could explain their complex biology. Isolating such complexes and determining their structures would further refine signaling mechanisms of this receptor. $GABA_B$ is also directly modulated by various toxins such as α-conotoxin, derived from the venom of marine snails of the *Conus* genus, which has been identified as a potential analgesic (*119*). It is completely unknown how these toxins are binding to $GABA_B$, which will be a matter of future biochemical and structural investigations.

All structures described in this review represent hetero- or homodimers. However, $GABA_B$ is also known to form higher-order oligomers such as tetramers (*56*). Future studies will be required to find out how these oligomers can be stabilized, as upon detergent solubilization, most of the receptors regress to their dimeric state. Another interesting avenue are heterodimers between different types of receptors, such as GB1 and CaSR, which have been described recently (*120*).

Last, while structural snapshots provide important high-resolution static views of stable conformational states and complexes, our understanding of the receptor function is incomplete without information about receptor dynamics, obtained by complementary spectroscopic techniques (*121*). Recent advancements in sample preparation and labeling methods as well as in single-molecule fluorescence, NMR, electron paramagnetic resonance, and computer modeling approaches should translate into accumulation of data on each state's free energy, dwell time, and exchange rates, providing a comprehensive view of the receptor's free energy landscape (*122*). Ultimately, time-resolved serial femtosecond crystallography at x-ray–free electron sources shows promise to record molecular movies of proteins undergoing conformational changes with high spatial and temporal resolution (*123*, *124*). Taking it all together, we expect that our understanding of $GABA_B$ function will advance to a new level within the next few years.

Note added in proof: a high resolution cryo-EM structure of GABAB-Gi complex is now available (https://doi.org/10.1038/s41586-021-03507-1).

REFERENCES AND NOTES

1. N. G. Bowery, B. Bettler, W. Froestl, J. P. Gallagher, F. Marshall, M. Raiteri, T. I. Bonner, S. J. Enna, International union of pharmacology. XXXIII. Mammalian γ-aminobutyric acid$_B$ receptors: Structure and function. *Pharmacol. Rev.* **54**, 247–264 (2002).
2. W. Sieghart, Structure, pharmacology, and function of $GABA_A$ receptor subtypes. *Adv. Pharmacol.* **54**, 231–263 (2006).
3. I. Soltesz, I. Mody, Patch-clamp recordings reveal powerful GABAergic inhibition in dentate hilar neurons. *J. Neurosci.* **14**, 2365–2376 (1994).
4. T. S. Otis, Y. De Koninck, I. Mody, Characterization of synaptically elicited GABAB responses using patch-clamp recordings in rat hippocampal slices. *J. Physiol.* **463**, 391–407 (1993).
5. M. Gassmann, B. Bettler, Regulation of neuronal $GABA_B$ receptor functions by subunit composition. *Nat. Rev. Neurosci.* **13**, 380–394 (2012).
6. V. Schuler, C. Lüscher, C. Blanchet, N. Klix, G. Sansig, K. Klebs, M. Schmutz, J. Heid, C. Gentry, L. Urban, Epilepsy, hyperalgesia, impaired memory, and loss of pre-and postsynaptic $GABA_B$ responses in mice lacking $GABA_{B(1)}$. *Neuron* **31**, 47–58 (2001).
7. E. Y. Chang, N. Ghosh, D. Yanni, S. Lee, D. Alexandru, T. Mozaffar, A review of spasticity treatments: Pharmacological and interventional approaches. *Crit. Rev. Phys. Rehabil. Med.* **25**, 11–22 (2013).
8. O. F. O'Leary, D. Felice, S. Galimberti, H. M. Savignac, J. A. Bravo, T. Crowley, M. El Yacoubi, J.-M. Vaugeois, M. Gassmann, B. Bettler, $GABA_{B(1)}$ receptor subunit isoforms differentially regulate stress resilience. *Proc. Natl. Acad. Sci. U.S.A.* **111**, 15232–15237 (2014).
9. I. Lapin, Phenibut (β-phenyl-GABA): A tranquilizer and nootropic drug. *CNS Drug Rev.* **7**, 471–481 (2001).
10. M. Malcangio, $GABA_B$ receptors and pain. *Neuropharmacology* **136**, 102–105 (2018).
11. M. Frankowska, M. Filip, E. Przegaliński, Effects of $GABA_B$ receptor ligands in animal tests of depression and anxiety. *Pharmacol. Rep.* **59**, 645–655 (2007).
12. M. S. Cousins, D. C. S. Roberts, H. de Wit, $GABA_B$ receptor agonists for the treatment of drug addiction: A review of recent findings. *Drug Alcohol Depend.* **65**, 209–220 (2002).
13. L. Chun, W. Zhang, J.-f. Liu, Structure and ligand recognition of class C GPCRs. *Acta Pharmacol. Sin.* **33**, 312–323 (2012).
14. J. H. White, A. Wise, M. J. Main, A. Green, N. J. Fraser, G. H. Disney, A. A. Barnes, P. Emson, S. M. Foord, F. H. Marshall, Heterodimerization is required for the formation of a functional $GABA_B$ receptor. *Nature* **396**, 679–682 (1998).
15. K. A. Jones, B. Borowsky, J. A. Tamm, D. A. Craig, M. M. Durkin, M. Dai, W.-J. Yao, M. Johnson, C. Gunwaldsen, L.-Y. Huang, C. Tang, Q. Shen, J. A. Salon, K. Morse, T. Laz, K. E. Smith, D. Nagarathnam, S. A. Noble, T. A. Branchek, C. Gerald, $GABA_B$ receptors function as a heteromeric assembly of the subunits $GABA_B$R1 and $GABA_B$R2. *Nature* **396**, 674–679 (1998).
16. K. Kaupmann, B. Malitschek, V. Schuler, J. Heid, W. Froestl, P. Beck, J. Mosbacher, S. Bischoff, A. Kulik, R. Shigemoto, A. Karschin, B. Bettler, $GABA_B$-receptor subtypes assemble into functional heteromeric complexes. *Nature* **396**, 683–687 (1998).
17. The UniProt Consortium, UniProt: A worldwide hub of protein knowledge. *Nucleic Acids Res.* **47**, D506–D515 (2019).
18. S. Hannan, M. E. Wilkins, T. G. Smart, Sushi domains confer distinct trafficking profiles on $GABA_B$ receptors. *Proc. Natl. Acad. Sci. U.S.A.* **109**, 12171–12176 (2012).
19. M. C. Dinamarca, A. Raveh, A. Schneider, T. Fritzius, S. Früh, P. D. Rem, M. Stawarski, T. Lalanne, R. Turecek, M. Choo, V. Besseyrias, W. Bildl, D. Bentrop, M. Staufenbiel, M. Gassmann, B. Fakler, J. Schwenk, B. Bettler, Complex formation of APP with $GABA_B$ receptors links axonal trafficking to amyloidogenic processing. *Nat. Commun.* **10**, 1331 (2019).
20. S. Burmakina, Y. Geng, Y. Chen, Q. R. Fan, Heterodimeric coiled-coil interactions of human $GABA_B$ receptor. *Proc. Natl. Acad. Sci. U.S.A.* **111**, 6958–6953 (2014).
21. L. Xue, Q. Sun, H. Zhao, X. Rovira, S. Gai, Q. He, J.-P. Pin, J. Liu, P. Rondard, Rearrangement of the transmembrane domain interfaces associated with the activation of a GPCR hetero-oligomer. *Nat. Commun.* **10**, 2765 (2019).
22. H. Shaye, A. Ishchenko, J. H. Lam, G. W. Han, L. Xue, P. Rondard, J. P. Pin, V. Katritch, C. Gati, V. Cherezov, Structural basis of the activation of a metabotropic GABA receptor. *Nature* **584**, 298–303 (2020).
23. J. Park, Z. Fu, A. Frangaj, J. Liu, L. Mosyak, T. Shen, V. N. Slavkovich, K. M. Ray, J. Taura, B. Cao, Y. Geng, H. Zuo, Y. Kou, R. Grassucci, S. Chen, Z. Liu, X. Lin, J. P. Williams, W. J. Rice, E. T. Eng, R. K. Huang, R. K. Soni, B. Kloss, Z. Yu, J. A. Javitch, W. A. Hendrickson,

P. A. Slesinger, M. Quick, J. Graziano, H. Yu, O. Fiehn, O. B. Clarke, J. Frank, Q. R. Fan, Structure of human $GABA_B$ receptor in an inactive state. *Nature* **584**, 304–309 (2020).
24. M. M. Papasergi-Scott, M. J. Robertson, A. B. Seven, O. Panova, J. M. Mathiesen, G. Skiniotis, Structures of metabotropic $GABA_B$ receptor. *Nature* **584**, 310–314 (2020).
25. C. Mao, C. Shen, C. Li, D.-D. Shen, C. Xu, S. Zhang, R. Zhou, Q. Shen, L.-N. Chen, Z. Jiang, J. Liu, Y. Zhang, Cryo-EM structures of inactive and active $GABA_B$ receptor. *Cell Res.* **30**, 564–573 (2020).
26. Y. Kim, E. Jeong, J.-H. Jeong, Y. Kim, Y. Cho, Structural basis for activation of the heterodimeric $GABA_B$ receptor. *J. Mol. Biol.* **432**, 5966–5984 (2020).
27. C. N. Kent, C. Park, C. W. Lindsley, Classics in chemical neuroscience: Baclofen. *ACS Chem. Nerosci.* **11**, 1740–1755 (2020).
28. E. Roberts, S. Frankel, γ-Aminobutyric acid in brain: Its formation from glutamic acid. *J. Biol. Chem.* **187**, 55–63 (1950).
29. J. Awapara, A. J. Landua, R. Fuerst, B. Seale, Free γ-aminobutyric acid in brain. *J. Biol. Chem.* **187**, 35–39 (1950).
30. A. W. Bazemore, K. A. C. Elliott, E. Florey, Isolation of factor I. *J. Neurochem.* **1**, 334–339 (1957).
31. K. Krnjević, S. Schwartz, The action of γ-aminobutyric acid on cortical neurones. *Exp. Brain Res.* **3**, 320–336 (1967).
32. N. G. Bowery, D. R. Hill, A. L. Hudson, A. Doble, D. N. Middlemiss, J. Shaw, M. Turnbull, (–) Baclofen decreases neurotransmitter release in the mammalian CNS by an action at a novel GABA receptor. *Nature* **283**, 92–94 (1980).
33. D. R. Hill, N. G. Bowery, ^{3}H-baclofen and ^{3}H-GABA bind to bicuculline-insensitive $GABA_B$ sites in rat brain. *Nature* **290**, 149–152 (1981).
34. P. Dutar, R. A. Nicoll, A physiological role for $GABA_B$ receptors in the central nervous system. *Nature* **332**, 156–158 (1988).
35. Y. Geng, D. Xiong, L. Mosyak, D. L. Malito, J. Kniazeff, Y. Chen, S. Burmakina, M. Quick, M. Bush, J. A. Javitch, J.-P. Pin, Q. R. Fan, Structure and functional interaction of the extracellular domain of human $GABA_B$ receptor GBR2. *Nat. Neurosci.* **15**, 970–978 (2012).
36. Y. Geng, M. Bush, L. Mosyak, F. Wang, Q. R. Fan, Structural mechanism of ligand activation in human $GABA_B$ receptor. *Nature* **504**, 254–259 (2013).
37. S. Zheng, N. Abreu, J. Levitz, A. C. Kruse, Structural basis for KCTD-mediated rapid desensitization of $GABA_B$ signalling. *Nature* **567**, 127–131 (2019).
38. H. Zuo, I. Glaaser, Y. Zhao, I. Kurinov, L. Mosyak, H. Wang, J. Liu, J. Park, A. Frangaj, E. Sturchler, M. Zhou, P. McDonald, Y. Geng, P. A. Slesinger, Q. R. Fan, Structural basis for auxilary subunit KCTD16 regulation of the $GABA_B$ receptor. *Proc. Natl. Acad. Sci.U.S.A.* **116**, 8370–8379 (2019).
39. S. Blein, R. Ginham, D. Uhrin, B. O. Smith, D. C. Soares, S. Veltel, R. A. J. McIlhinney, J. H. White, P. N. Barlow, Structural analysis of the Complement Control Protein (CCP) Modules of $GABA_B$ Receptor 1a: Only one of the two CCP modules is compactly folded. *J. Biol. Chem.* **279**, 48292–48306 (2004).
40. H. C. Rice, D. De Malmazet, A. Schreurs, S. Frere, I. Van Molle, A. N. Volkov, E. Creemers, I. Vertkin, J. Nys, F. M. Ranaivoson, D. Comoletti, J. N. Savas, H. Remaut, D. Balschun, K. D. Wierda, I. Slutsky, K. Farrow, B. De Strooper, J. de Wit, Secreted amyloid-β precursor protein functions as a $GABA_B$R1a ligand to modulate synaptic transmission. *Science* **363**, eaao4827 (2019).
41. B. C. Choy, R. J. Cater, F. Mancia, E. E. Pryor Jr., A 10-year meta-analysis of membrane protein structural biology: Detergents, membrane mimetics, and structure determination techniques. *Biochim. Biophys. Acta Biomembr.* **1863**, 183533 (2021).
42. M. Schorb, I. Haberbosch, W. J. H. Hagen, Y. Schwab, D. N. Mastronarde, Software tools for automated transmission electron microscopy. *Nat. Methods* **16**, 471–477 (2019).
43. A. Punjani, H. Zhang, D. J. Fleet, Non-uniform refinement: Adaptive regularization improves single-particle cryo-EM reconstruction. *Nat. Methods* **17**, 1214–1221 (2020).
44. J. Zivanov, T. Nakane, S. H. W. Scheres, Estimation of high-order aberrations and anisotropic magnification from cryo-EM data sets in RELION-3.1. *IUCrJ* **7**, 253–267 (2020).
45. J. Zivanov, T. Nakane, S. H. W. Scheres, A Bayesian approach to beam-induced motion correction in cryo-EM single-particle analysis. *IUCrJ* **6**, 5–17 (2019).
46. J. Krushkal, O. Bat, I. Gigli, Evolutionary relationships among proteins encoded by the regulator of complement activation gene cluster. *Mol. Biol. Evol.* **17**, 1718–1730 (2000).
47. B. Zarzycka, S. A. Zaidi, B. L. Roth, V. Katritch, Harnessing ion-binding sites for GPCR pharmacology. *Pharmacol. Rev.* **71**, 571–595 (2019).
48. J. Yu, L. E. Gimenez, C. C. Hernandez, Y. Wu, A. H. Wein, G. W. Han, K. McClary, S. R. Mittal, K. Burdsall, B. Stauch, L. Wu, S. N. Stevens, A. Peisley, S. Y. Williams, V. Chen, G. L. Millhauser, S. Zhao, R. D. Cone, R. C. Stevens, Determination of the melanocortin-4 receptor structure identifies Ca^{2+} as a cofactor for ligand binding. *Science* **368**, 428–433 (2020).
49. K. Kato, M. Goto, H. Fukuda, Regulation by divalent cations of ^{3}H-baclofen binding to $GABA_B$ sites in rat cerebellar membranes. *Life Sci.* **32**, 879–887 (1983).
50. A. Wise, A. Green, M. J. Main, R. Wilson, N. Fraser, F. H. Marshall, Calcium sensing properties of the $GABA_B$ receptor. *Neuropharmacology* **38**, 1647–1656 (1999).
51. T. Galvez, S. Urwyler, L. Prézeau, J. Mosbacher, C. Joly, B. Malitschek, J. Heid, I. Brabet, W. Froestl, B. Bettler, K. Kaupmann, J.-P. Pin, Ca^{2+} requirement for high-affinity γ-aminobutyric acid (GABA) binding at $GABA_B$ receptors: Involvement of serine 269 of the $GABA_B$R1 subunit. *Mol. Pharmacol.* **57**, 419–426 (2000).
52. R. S. Mukherjee, E. W. McBride, M. Beinborn, K. Dunlap, A. S. Kopin, Point mutations in either subunit of the $GABA_B$ receptor confer constitutive activity to the heterodimer. *Mol. Pharmacol.* **70**, 1406–1413 (2006).
53. A. S. Doré, K. Okrasa, J. C. Patel, M. Serrano-Vega, K. Bennett, R. M. Cooke, J. C. Errey, A. Jazayeri, S. Khan, B. Tehan, M. Weir, G. R. Wiggin, F. H. Marshall, Structure of class C GPCR metabotropic glutamate receptor 5 transmembrane domain. *Nature* **511**, 557–562 (2014).
54. P. Malherbe, R. Masciadri, R. D. Norcross, F. Knoflach, C. Kratzeisen, M.-T. Zenner, Y. Kolb, A. Marcuz, J. Huwyler, T. Nakagawa, R. H. P. Porter, A. W. Thomas, J. G. Wettstein, A. J. Sleight, W. Spooren, E. P. Prinssen, Characterization of (*R*,*S*)-5, 7-di-*tert*-butyl-3-hydroxy-3-trifluoromethyl-3*H*-benzofuran-2-one as a positive allosteric modulator of $GABA_B$ receptors. *Br. J. Pharmacol.* **154**, 797–811 (2008).
55. J.-F. Villemure, L. Adam, N. J. Bevan, K. Gearing, S. Chénier, M. Bouvier, Subcellular distribution of $GABA_B$ receptor homo-and hetero-dimers. *Biochem. J.* **388**, 47–55 (2005).
56. L. Comps-Agrar, J. Kniazeff, L. Nørskov-Lauritsen, D. Maurel, M. Gassmann, N. Gregor, L. Prézeau, B. Bettler, T. Durroux, E. Trinquet, J.-P. Pin, The oligomeric state sets $GABA_B$ receptor signalling efficacy. *EMBO J.* **30**, 2336–2349 (2011).
57. A. Ellaithy, J. Gonzalez-Maeso, D. A. Logothetis, J. Levitz, Structural and biophysical mechanisms of class CG protein-coupled receptor function. *Trends Biochem. Sci.* **45**, 1049–1064 (2020).
58. E. O. Grushevskyi, T. Kukaj, R. Schmauder, A. Bock, U. Zabel, T. Schwabe, K. Benndorf, M. J. Lohse, Stepwise activation of a class C GPCR begins with millisecond dimer rearrangement. *Proc. Natl. Acad. Sci. U.S.A.* **116**, 10150–10155 (2019).
59. J. Levitz, C. Habrian, S. Bharill, Z. Fu, R. Vafabakhsh, E. Y. Isacoff, Mechanism of assembly and cooperativity of homomeric and heteromeric metabotropic glutamate receptors. *Neuron* **92**, 143–159 (2016).
60. N. Lecat-Guillet, C. Monnier, X. Rovira, J. Kniazeff, L. Lamarque, J. M. Zwier, E. Trinquet, J.-P. Pin, P. Rondard, FRET-based sensors unravel activation and allosteric modulation of the $GABA_B$ receptor. *Cell Chem. Biol.* **24**, 360–370 (2017).
61. J.-P. Pin, B. Bettler, Organization and functions of mGlu and $GABA_B$ receptor complexes. *Nature* **540**, 60–68 (2016).
62. E. H. Schneider, D. Schnell, A. Strasser, S. Dove, R. Seifert, Impact of the DRY motif and the missing "ionic lock" on constitutive activity and G-protein coupling of the human histamine H_4 receptor. *J. Pharmacol. Exp. Ther.* **333**, 382–392 (2010).
63. V. Binet, B. Duthey, J. Lecaillon, C. Vol, J. Quoyer, G. Labesse, J.-P. Pin, L. Prézeau, Common structural requirements for heptahelical domain function in class A and class C G protein-coupled receptors. *J. Biol. Chem.* **282**, 12154–12163 (2007).
64. V. Isberg, C. de Graaf, A. Bortolato, V. Cherezov, V. Katritch, F. H. Marshall, S. Mordalski, J.-P. Pin, R. C. Stevens, G. Vriend, D. E. Gloriam, Generic GPCR residue numbers–aligning topology maps while minding the gaps. *Trends Pharmacol. Sci.* **36**, 22–31 (2015).
65. T. W. Schwartz, T. M. Frimurer, B. Holst, M. M. Rosenkilde, C. E. Elling, Molecular mechanism of 7TM receptor activation—A global toggle switch model. *Annu. Rev. Pharmacol. Toxicol.* **46**, 481–519 (2006).
66. B. Trzaskowski, D. Latek, S. Yuan, U. Ghoshdastider, A. Debinski, S. Filipek, Action of molecular switches in GPCRs-theoretical and experimental studies. *Curr. Med. Chem.* **19**, 1090–1109 (2012).
67. J. Cao, S. Huang, J. Qian, J. Huang, L. Jin, Z. Su, J. Yang, J. Liu, Evolution of the class C GPCR Venus flytrap modules involved positive selected functional divergence. *BMC Evol. Biol.* **9**, 67 (2009).
68. A. D. Yates, P. Achuthan, W. Akanni, J. Allen, J. Allen, J. Alvarez-Jarreta, M. R. Amode, I. M. Armean, A. G. Azov, R. Bennett, J. Bhai, K. Billis, S. Boddu, J. C. Marugán, C. Cummins, C. Davidson, K. Dodiya, R. Fatima, A. Gall, C. G. Giron, L. Gil, T. Grego, L. Haggerty, E. Haskell, T. Hourlier, O. G. Izuogu, S. H. Janacek, T. Juettemann, M. Kay, I. Lavidas, T. Le, D. Lemos, J. G. Martinez, T. Maurel, M. McDowall, A. McMahon, S. Mohanan, B. Moore, M. Nuhn, D. N. Oheh, A. Parker, A. Parton, M. Patricio, M. P. Sakthivel, A. I. A. Salam, B. M. Schmitt, H. Schuilenburg, D. Sheppard, M. Sycheva, M. Szuba, K. Taylor, A. Thormann, G. Threadgold, A. Vullo, B. Walts, A. Winterbottom, A. Zadissa, M. Chakiachvili, B. Flint, A. Frankish, S. E. Hunt, G. Ilsley, M. Kostadima, N. Langridge, J. E. Loveland, F. J. Martin, J. Morales, J. M. Mudge, M. Muffato, E. Perry, M. Ruffier, S. J. Trevanion, F. Cunningham, K. L. Howe, D. R. Zerbino, P. Flicek, Ensembl 2020. *Nucleic Acids Res.* **48**, D682–D688 (2020).
69. K. J. Karczewski, L. C. Francioli, G. Tiao, B. B. Cummings, J. Alföldi, Q. Wang, R. L. Collins, K. M. Laricchia, A. Ganna, D. P. Birnbaum, L. D. Gauthier, H. Brand, M. Solomonson, N. A. Watts, D. Rhodes, M. Singer-Berk, E. M. England, E. G. Seaby, J. A. Kosmicki, R. K. Walters, K. Tashman, Y. Farjoun, E. Banks, T. Poterba, A. Wang, C. Seed, N. Whiffin, J. X. Chong, K. E. Samocha, E. Pierce-Hoffman, Z. Zappala, A. H. O'Donnell-Luria, E. V. Minikel, B. Weisburd, M. Lek, J. S. Ware, C. Vittal, I. M. Armean, L. Bergelson, K. Cibulskis, K. M. Connolly, M. Covarrubias, S. Donnelly, S. Ferriera, S. Gabriel, J. Gentry, N. Gupta, T. Jeandet, D. Kaplan, C. Llanwarne, R. Munshi, S. Novod, N. Petrillo, D. Roazen, V. Ruano-Rubio, A. Saltzman, M. Schleicher, J. Soto, K. Tibbetts, C. Tolonen, G. Wade,

M. E. Talkowski; Genome Aggregation Database Consortium, B. M. Neale, M. J. Daly, D. G. MacArthur, The mutational constraint spectrum quantified from variation in 141,456 humans. *Nature* **581**, 434–443 (2020).
70. K. E. Samocha, E. B. Robinson, S. J. Sanders, C. Stevens, A. Sabo, L. M. McGrath, J. A. Kosmicki, K. Rehnström, S. Mallick, A. Kirby, D. P. Wall, D. G. MacArthur, S. B. Gabriel, M. De Pristo, S. M. Purcell, A. Palotie, E. Boerwinkle, J. D. Buxbaum, E. H. Cook Jr., R. A. Gibbs, G. D. Schellenberg, J. S. Sutcliffe, B. Devlin, K. Roeder, B. M. Neale, M. J. Daly, A framework for the interpretation of de novo mutation in human disease. *Nat. Genet.* **46**, 944–950 (2014).
71. M. Lek, K. J. Karczewski, E. V. Minikel, K. E. Samocha, E. Banks, T. Fennell, A. H. O'Donnell-Luria, J. S. Ware, A. J. Hill, B. B. Cummings, T. Tukiainen, D. P. Birnbaum, J. A. Kosmicki, L. E. Duncan, K. Estrada, F. Zhao, J. Zou, E. Pierce-Hoffman, J. Berghout, D. N. Cooper, N. Deflaux, M. De Pristo, R. Do, J. Flannick, M. Fromer, L. Gauthier, J. Goldstein, N. Gupta, D. Howrigan, A. Kiezun, M. I. Kurki, A. L. Moonshine, P. Natarajan, L. Orozco, G. M. Peloso, R. Poplin, M. A. Rivas, V. Ruano-Rubio, S. A. Rose, D. M. Ruderfer, K. Shakir, P. D. Stenson, C. Stevens, B. P. Thomas, G. Tiao, M. T. Tusie-Luna, B. Weisburd, H.-H. Won, D. Yu, D. M. Altshuler, D. Ardissino, M. Boehnke, J. Danesh, S. Donnelly, R. Elosua, J. C. Florez, S. B. Gabriel, G. Getz, S. J. Glatt, C. M. Hultman, S. Kathiresan, M. Laakso, S. McCarroll, M. I. McCarthy, D. McGovern, R. McPherson, B. M. Neale, A. Palotie, S. M. Purcell, D. Saleheen, J. M. Scharf, P. Sklar, P. F. Sullivan, J. Tuomilehto, M. T. Tsuang, H. C. Watkins, J. G. Wilson, M. J. Daly, D. G. MacArthur; Exome Aggregation Consortium, Analysis of protein-coding genetic variation in 60,706 humans. *Nature* **536**, 285–291 (2016).
72. F. F. Hamdan, C. T. Myers, P. Cossette, P. Lemay, D. Spiegelman, A. D. Laporte, C. Nassif, O. Diallo, J. Monlong, M. Cadieux-Dion, S. Dobrzeniecka, C. Meloche, K. Retterer, M. T. Cho, J. A. Rosenfeld, W. Bi, C. Massicotte, M. Miguet, L. Brunga, B. M. Regan, K. Mo, C. Tam, A. Schneider, G. Hollingsworth; Deciphering Developmental Disorders Study, D. R. FitzPatrick, A. Donaldson, N. Canham, E. Blair, B. Kerr, A. E. Fry, R. H. Thomas, J. Shelagh, J. A. Hurst, H. Brittain, M. Blyth, R. R. Lebel, E. H. Gerkes, L. Davis-Keppen, Q. Stein, W. K. Chung, S. J. Dorison, P. J. Benke, E. Fassi, N. Corsten-Janssen, E.-J. Kamsteeg, F. T. Mau-Them, A.-L. Bruel, A. Verloes, K. Ounap, M. H. Wojcik, D. V. F. Albert, S. Venkateswaran, T. Ware, D. Jones, Y.-C. Liu, S. S. Mohammad, P. Bizargity, C. A. Bacino, V. Leuzzi, S. Martinelli, B. Dallapiccola, M. Tartaglia, L. Blumkin, K. J. Wierenga, G. Purcarin, J. J. O'Byrne, S. Stockler, A. Lehman, B. Keren, M.-C. Nougues, C. Mignot, S. Auvin, C. Nava, S. M. Hiatt, M. Bebin, Y. Shao, F. Scaglia, S. R. Lalani, R. E. Frye, I. T. Jarjour, S. Jacques, R.-M. Boucher, E. Riou, M. Srour, L. Carmant, A. Lortie, P. Major, P. Diadori, F. Dubeau, G. D'Anjou, G. Bourque, S. F. Berkovic, L. G. Sadleir, P. M. Campeau, Z. Kibar, R. G. Lafrenière, S. L. Girard, S. Mercimek-Mahmutoglu, C. Boelman, G. A. Rouleau, I. E. Scheffer, H. C. Mefford, D. M. Andrade, E. Rossignol, B. A. Minassian, J. L. Michaud, High rate of recurrent de novo mutations in developmental and epileptic encephalopathies. *Am. J. Hum. Genet.* **101**, 664–685 (2017).
73. Y. Yoo, J. Jung, Y.-N. Lee, Y. Lee, H. Cho, E. Na, J. Y. Hong, E. Kim, J. S. Lee, J. S. Lee, C. Hong, S.-Y. Park, J. Wie, K. Miller, N. Shur, C. Clow, R. S. Ebel, S. D. De Brosse, L. B. Henderson, R. Willaert, C. Castaldi, I. Tikhonova, K. Bilgüvar, S. Mane, K. J. Kim, Y. S. Hwang, S.-G. Lee, I. So, B. C. Lim, H.-J. Choi, J. Y. Seong, Y. B. Shin, H. Jung, J.-H. Chae, M. Choi, GABBR2 mutations determine phenotype in rett syndrome and epileptic encephalopathy. *Ann. Neurol.* **82**, 466–478 (2017).
74. M.-L. Vuillaume, M. Jeanne, L. Xue, S. Blesson, A.-S. Denomme-Pichon, S. Alirol, C. Brulard, E. Colin, B. Isidor, B. Gilbert-Dussardier, S. Odent, P. Parent, A. Donnart, R. Redon, S. Bézieau, P. Rondard, F. Laumonnier, A. Toutain, A novel mutation in the transmembrane 6 domain of GABBR2 leads to a Rett-like phenotype. *Ann. Neurol.* **83**, 437–439 (2018).
75. M. Jazvinscak Jembrek, J. Vlainic, GABA receptors: Pharmacological potential and pitfalls. *Curr. Pharm. Des.* **21**, 4943–4959 (2015).
76. E. Sigel, M. Ernst, The benzodiazepine binding sites of $GABA_A$ receptors. *Trends Pharmacol. Sci.* **39**, 659–671 (2018).
77. R. W. Olsen, $GABA_A$ receptor: Positive and negative allosteric modulators. *Neuropharmacology* **136**, 10–22 (2018).
78. E. Boonstra, R. de Kleijn, L. S. Colzato, A. Alkemade, B. U. Forstmann, S. Nieuwenhuis, Neurotransmitters as food supplements: The effects of GABA on brain and behavior. *Front. Psychol.* **6**, 1520 (2015).
79. W. Froestl, Chemistry and pharmacology of $GABA_B$ receptor ligands. *Adv. Pharmacol.* **58**, 19–62 (2010).
80. H. Keberle, J. W. Faigle, M. Wilhelm, Procedure for the preparation of new amino acids, Swiss Patent 449046, Publication Date: 11 Apr 1968, Priority: 09 Jul 1963. *Chem. Abstr.* **69**, 106273f (1968).
81. D. R. Curtis, D. Lodge, J. C. Bornstein, M. J. Peet, Selective effects of (−)-baclofen on spinal synaptic transmission in the cat. *Exp. Brain Res.* **42**, 158–170 (1981).
82. W. Froestl, S. J. Mickel, R. G. Hall, G. von Sprecher, D. Strub, P. A. Baumann, F. Brugger, C. Gentsch, J. Jaekel, Phosphinic acid analogs of GABA. 1. New potent and selective GABAB agonists. *J. Med. Chem.* **38**, 3297–3312 (1995).
83. J. B. M. M. van Bree, C. D. Heijligers-Feijen, A. G. de Boer, M. Danhof, D. D. Breimer, Stereoselective transport of baclofen across the blood–brain barrier in rats as determined by the unit impulse response methodology. *Pharm. Res.* **8**, 259–262 (1991).
84. R. Lal, J. Sukbuntherng, E. H. L. Tai, S. Upadhyay, F. Yao, M. S. Warren, W. Luo, L. Bu, S. Nguyen, J. Zamora, G. Peng, T. Dias, Y. Bao, M. Ludwikow, T. Phan, R. A. Scheuerman, H. Yan, M. Gao, Q. Q. Wu, T. Annamalai, S. P. Raillard, K. Koller, M. A. Gallop, K. C. Cundy, Arbaclofen placarbil, a novel *R*-baclofen prodrug: Improved absorption, distribution, metabolism, and elimination properties compared with R-baclofen. *J. Pharmacol. Exp. Ther.* **330**, 911–921 (2009).
85. G. Bartholini, B. Scatton, B. Zivkovic, Effect of the new gamma-aminobutyric acid agonist SL 76 002 on striatal acetylcholine: Relation to neuroleptic-induced extrapyramidal alterations. *Adv. Biochem. Psychopharmacol.* **24**, 207–213 (1980).
86. V. M. Kopelevich, V. I. Gunar, Some approaches to the directed search for new drugs based on nicotinic acid. *Pharm. Chem. J.* **33**, 177–187 (1999).
87. K. Matsuyama, C. Yamashita, A. Noda, S. Goto, H. Noda, Y. Ichimaru, Y. Gomita, Evaluation of isonicotinoyl-γ-aminobutyric acid (GABA) and nicotinoyl-GABA as pro-drugs of GABA. *Chem. Pharm. Bull.* **32**, 4089–4095 (1984).
88. Y. Geffen, R. Keefe, J. Rabinowitz, R. Anand, M. Davidson, BL-1020, a new γ-aminobutyric acid–enhanced antipsychotic: Results of 6-week, randomized, double-blind, controlled, efficacy and safety study. *J. Clin. Psychiatry* **73**, e1168–e1174 (2012).
89. A. Nudelman, I. Gil-Ad, N. Shpaisman, I. Terasenko, H. Ron, K. Savitsky, Y. Geffen, A. Weizman, A. Rephaeli, A mutual prodrug ester of GABA and perphenazine exhibits antischizophrenic efficacy with diminished extrapyramidal effects. *J. Med. Chem.* **51**, 2858–2862 (2008).
90. L. P. Carter, W. Koek, C. P. France, Behavioral analyses of GHB: Receptor mechanisms. *Pharmacol. Ther.* **121**, 100–114 (2009).
91. W. Chen, H. Wu, R. J. Hernandez, A. K. Mehta, M. K. Ticku, C. P. France, A. Coop, Ethers of 3-hydroxyphenylacetic acid as selective gamma-hydroxybutyric acid receptor ligands. *Bioorg. Med. Chem. Lett.* **15**, 3201–3202 (2005).
92. Y. Wu, S. Ali, G. Ahmadian, C. C. Liu, Y. T. Wang, K. M. Gibson, A. R. Calver, J. Francis, M. N. Pangalos, O. C. Snead III, γ-Hydroxybutyric acid (GHB) and γ-aminobutyric $acid_B$ receptor ($GABA_BR$) binding sites are distinctive from one another: Molecular evidence. *Neuropharmacology* **47**, 1146–1156 (2004).
93. C. Andriamampandry, O. Taleb, V. Kemmel, J.-P. Humbert, D. Aunis, M. Maitre, Cloning and functional characterization of a gamma-hydroxybutyrate receptor identified in the human brain. *FASEB J.* **21**, 885–895 (2007).
94. E. J. M. Mignot, A practical guide to the therapy of narcolepsy and hypersomnia syndromes. *Neurotherapeutics* **9**, 739–752 (2012).
95. E. Szabadi, GHB for cataplexy: Possible mode of action. *J. Psychopharmacol.* **29**, 744–749 (2015).
96. A. J. Bredenoord, Lesogaberan, a GABA(B) agonist for the potential treatment of gastroesophageal reflux disease. *IDrugs* **12**, 576–584 (2009).
97. S. Ghose, M. K. Winter, K. E. McCarson, C. A. Tamminga, S. J. Enna, The GABAB receptor as a target for antidepressant drug action. *Br. J. Pharmacol.* **162**, 1–17 (2011).
98. S. J. Enna, GABAB receptor agonists and antagonists: Pharmacological properties and therapeutic possibilities. *Expert Opin. Investig. Drugs* **6**, 1319–1325 (1997).
99. D. I. B. Kerr, J. Ong, C. Vaccher, P. Berthelot, N. Flouquet, M.-P. Vaccher, M. Debaert, GABAB receptor antagonism by resolved (R)-saclofen in the guinea-pig ileum. *Eur. J. Pharmacol.* **308**, R1–R2 (1996).
100. D. I. B. Kerr, J. Ong, D. J. Doolette, K. Schafer, R. H. Prager, The (S)-enantiomer of 2-hydroxysaclofen is the active GABAB receptor antagonist in central and peripheral preparations. *Eur. J. Pharmacol.* **287**, 185–189 (1995).
101. D. I. B. Kerr, J. Ong, R. H. Prager, B. D. Gynther, D. R. Curtis, Phaclofen: A peripheral and central baclofen antagonist. *Brain Res.* **405**, 150–154 (1987).
102. G. R. Seabrook, W. Howson, M. G. Lacey, Electrophysiological characterization of potent agonists and antagonists at pre-and postsynaptic GABAB receptors on neurones in rat brain slices. *Br. J. Pharmacol.* **101**, 949–957 (1990).
103. J. Ong, S. Bexis, V. Marino, D. A. S. Parker, D. I. B. Kerr, W. Froestl, CGP 36216 is a selective antagonist at GABAB presynaptic receptors in rat brain. *Eur. J. Pharmacol.* **415**, 191–195 (2001).
104. W. Frostl, S. J. Mickel, G. Von Sprecher, P. J. Diel, R. G. Hall, L. Maier, D. Strub, V. Melillo, P. A. Baumann, R. Bernasconi, Phosphinic acid analogs of GABA. 2. Selective, orally active GABAB receptors. *J. Med. Chem.* **38**, 3313–3331 (1995).
105. W. Froestl, M. Gallagher, H. Jenkins, A. Madrid, T. Melcher, S. Teichman, C. G. Mondadori, R. Pearlman, SGS742: The first GABAB receptor antagonist in clinical trials. *Biochem. Pharmacol.* **68**, 1479–1487 (2004).
106. S. Gauthier, P. S. Aisen, S. H. Ferris, D. Saumier, A. Duong, D. Haine, D. Garceau, J. Suhy, J. Oh, W. Lau, J. Sampalis, Effect of tramiprosate in patients with mild-to-moderate Alzheimer's disease: Exploratory analyses of the MRI sub-group of the Alphase study. *J. Nutr. Health Aging* **13**, 550–557 (2009).
107. D. C. Bolser, D. J. Blythin, R. W. Chapman, R. W. Egan, J. A. Hey, C. Rizzo, S.-C. Kuo, W. Kreutner, The pharmacology of SCH 50911: A novel, orally-active GABA-beta receptor antagonist. *J. Pharmacol. Exp. Ther.* **274**, 1393–1398 (1995).

108. T. P. Kenakin, Biased signalling and allosteric machines: New vistas and challenges for drug discovery. *Br. J. Pharmacol.* **165**, 1659–1669 (2012).
109. H. Bittiger, N. Reymann, R. Hall, P. Kane, CGP27492, a new potent and selective radioligand for GABAB receptors. *Eur. J. Neurosci.* **16**, 10 (1988).
110. M. Chebib, R. J. Vandenberg, W. Froestl, G. A. R. Johnston, Unsaturated phosphinic analogues of γ-aminobutyric acid as GABAC receptor antagonists. *Eur. J. Pharmacol.* **329**, 223–229 (1997).
111. S. Patel, S. Naeem, A. Kesingland, W. Froestl, M. Capogna, L. Urban, A. Fox, The effects of GABAB agonists and gabapentin on mechanical hyperalgesia in models of neuropathic and inflammatory pain in the rat. *Pain* **90**, 217–226 (2001).
112. J.-P. Pin, L. Prézeau, Allosteric modulators of $GABA_B$ receptors: Mechanism of action and therapeutic perspective. *Curr. Neuropharmacol.* **5**, 195–201 (2007).
113. M. Filip, M. Frankowska, A. Sadakierska-Chudy, A. Suder, Ł. Szumiec, P. Mierzejewski, P. Bienkowski, E. Przegaliński, J. F. Cryan, GABAB receptors as a therapeutic strategy in substance use disorders: Focus on positive allosteric modulators. *Neuropharmacology* **88**, 36–47 (2015).
114. E. Augier, Recent advances in the potential of positive allosteric modulators of the GABAB receptor to treat alcohol use disorder. *Alcohol Alcohol.* **56**, 139–148 (2021).
115. S. Urwyler, J. Mosbacher, K. Lingenhoehl, J. Heid, K. Hofstetter, W. Froestl, B. Bettler, K. Kaupmann, Positive allosteric modulation of native and recombinant γ-aminobutyric acidB receptors by 2, 6-di-tert-butyl-4-(3-hydroxy-2, 2-dimethyl-propyl)-phenol (CGP7930) and its aldehyde analog CGP13501. *Mol. Pharmacol.* **60**, 963–971 (2001).
116. S. Urwyler, M. F. Pozza, K. Lingenhoehl, J. Mosbacher, C. Lampert, W. Froestl, M. Koller, K. Kaupmann, *N,N'*-Dicyclopentyl-2-methylsulfanyl-5-nitro-pyrimidine-4,6-diamine (GS39783) and Structurally Related Compounds: Novel Allosteric Enhancers of γ-Aminobutyric $Acid_B$ Receptor Function. *J. Pharmacol. Exp. Ther.* **307**, 322–330 (2003).
117. L.-H. Chen, B. Sun, Y. Zhang, T.-J. Xu, Z.-X. Xia, J.-F. Liu, F.-J. Nan, Discovery of a negative allosteric modulator of GABAB receptors. *ACS Med. Chem. Lett.* **5**, 742–747 (2014).
118. J. Schwenk, E. Pérez-Garci, A. Schneider, A. Kollewe, A. Gauthier-Kemper, T. Fritzius, A. Raveh, M. C. Dinamarca, A. Hanuschkin, W. Bildl, J. Klingauf, M. Gassmann, U. Schulte, B. Bettler, B. Fakler, Modular composition and dynamics of native $GABA_B$ receptors identified by high-resolution proteomics. *Nat. Neurosci.* **19**, 233–242 (2016).
119. M. Sadeghi, B. B. Carstens, B. P. Callaghan, J. T. Daniel, H.-S. Tae, T. O'Donnell, J. Castro, S. M. Brierley, D. J. Adams, D. J. Craik, R. J. Clark, Structure–activity studies reveal the molecular basis for $GABA_B$-receptor mediated inhibition of high voltage-activated calcium channels by α-conotoxin Vc1. 1. *ACS Chem. Biol.* **13**, 1577–1587 (2018).
120. W. Chang, C.-L. Tu, F. G. Jean-Alphonse, A. Herberger, Z. Cheng, J. Hwong, H. Ho, A. Li, D. Wang, H. Liu, A. D. White, I. Suh, W. Shen, Q.-Y. Duh, E. Khanafshar, D. M. Shoback, K. Xiao, J.-P. Vilardaga, PTH hypersecretion triggered by a $GABA_{B1}$ and Ca^{2+}-sensing receptor heterocomplex in hyperparathyroidism. *Nat. Metab.* **2**, 243–255 (2020).
121. A. Gusach, I. Maslov, A. Luginina, V. Borshchevskiy, A. Mishin, V. Cherezov, Beyond structure: Emerging approaches to study GPCR dynamics. *Curr. Opin. Struct. Biol.* **63**, 18–25 (2020).
122. X. Deupi, B. K. Kobilka, Energy landscapes as a tool to integrate GPCR structure, dynamics, and function. *Phys. Ther.* **25**, 293–303 (2010).
123. B. Stauch, V. Cherezov, Serial femtosecond crystallography of G protein–coupled receptors. *Annu. Rev. Biophys.* **47**, 377–397 (2018).
124. L. C. Johansson, B. Stauch, A. Ishchenko, V. Cherezov, A bright future for serial femtosecond crystallography with XFELs. *Trends Biochem. Sci.* **42**, 749–762 (2017).
125. D. Eisenberg, E. Schwarz, M. Komarony, R. Wall, Amino acid scale: Normalized consensus hydrophobicity scale. *J. Mol. Biol.* **179**, 125–142 (1984).
126. A. P. Bento, A. Gaulton, A. Hersey, L. J. Bellis, J. Chambers, M. Davies, F. A. Krüger, Y. Light, L. Mak, S. McGlinchey, M. Nowotka, G. Papadatos, R. Santos, J. P. Overington, The ChEMBL bioactivity database: An update. *Nucleic Acids Res.* **42**, D1083–D1090 (2014).
127. S. Kim, J. Chen, T. Cheng, A. Gindulyte, J. He, S. He, Q. Li, B. A. Shoemaker, P. A. Thiessen, B. Yu, L. Zaslavsky, J. Zhang, E. E. Bolton, PubChem 2019 update: Improved access to chemical data. *Nucleic Acids Res.* **47**, D1102–D1109 (2019).

Acknowledgment: We thank Y. Kadyshevskaya for the help with preparing illustrations. **Funding:** This work was supported by a grant from the National Institute of General Medical Sciences (R35 GM127086). **Author contributions:** All authors contributed to writing the manuscript. H.S., B.S., and V.C. prepared illustrations. All authors approved the final draft. **Competing interests:** The authors declare that they have no competing interests. **Data and materials availability:** All data needed to evaluate the conclusions in the paper are present in the paper and/or in the materials cited herein.

Submitted 28 December 2020
Accepted 14 April 2021
Published 28 May 2021
10.1126/sciadv.abg3362

Citation: H. Shaye, B. Stauch, C. Gati, V. Cherezov, Molecular mechanisms of metabotropic $GABA_B$ receptor function. *Sci. Adv.* **7**, eabg3362 (2021).